THE LEAF VENATION AND REPRODUCTIVE STRUCTURES OF A LATE TRIASSIC ANGIOSPERM, SANMIGUELIA LEWISII

BRUCE CORNET
14222 Kimberley Ln., #411
Houston, TX 77079
Received 17 June 1986, 26 August 1986

ABSTRACT: An *in situ* vegetative colony of *Sanmiguelia lewisii* Brown with organic remains preserved is described from the Late Carnian upper Trujillo Formation of the Dockum Group in northwestern Texas. Well preserved leaves, leaf venation, stems, roots, rhizomes, and their anatomy, reproductive branch systems, their megasporophylls and microsporophylls, ovules, seeds, and pollen provide abundant new evidence to interpret the systematic affinities of this controversial Late Triassic plant. The vegetative and reproductive organs of *S. lewisii* emended are decribed in detail, with anatomical information included secondarily. Leaves possess four orders of poorly organized parallel venation, abundant cross veins, and apical vein fusion, and show evidence of intercalary growth. Carpel-like megasporophylls (*Axelrodia burgeri* Cornet gen. et sp. nov.) with apical stigma-like organs are borne individually on tertiary branches and at the ends of secondary branches in flower-like clusters on a paniculate inflorescence with sheathing cataphylls, subtended by a large spathe-like vegetative leaf. Paired sessile biloculate anther-like microsporophylls (*Synangispadixis tidwellii* Cornet gen. et sp. nov.) containing tectate-granular monosulcate pollen were borne in synangia along a spadix-like inflorescence, probably also subtended by a large spathe-like leaf. *A. burgeri* contains paired anatropous ovules enclosed in an ovary, and large bean-shaped seeds (identical to the dispersed seeds, *Nemececkigone fabaforma* Cornet gen. et sp. nov.) that developed late in megasporophyll development, and contain a dicotyledonous embryo with one cotyledon significantly larger than the other. Axes of *S. lewisii* have vesselless secondary xylem containing tracheids with helical-scalariform and circular bordered pits, uniseriate rays and vascular leaf traces that occupied giant multiseriate rays or wood gaps. The secondary xylem of the primary root system contains vessels. *S. lewisii* is compared with angiosperm-like fruiting structures from Carnian strata of the Richmond

****

This paper is dedicated to my wife, Bonnie Lee Cornet, whose love, inspiration, and patience helped make this manuscript possible. The author wishes to acknowledge the following people for their help in finding and in collecting specimens at the Sunday Canyon locality: Drs. S.R. Ash, P.A. Murry, P.E. Olsen, and D.L. Dilcher, and the field assistance of A. Santa Luca and A.J. Litt. He also wishes to acknowledge the local geologic and paleontologic knowledge provided by P.A. Murry and P.E. Olsen, and the discussions, support, and advice of W.C. Burger and the late G.R. Fournier. The author acknowledges The Pennsylvania State University (N.S.F. grant no. GA36870 to Professor Alfred Traverse), the Philadelphia Academy of Natural Sciences, the late Gulf Research & Development Co., and Exxon Co. U.S.A. for the facilities, equipment, and materials that together made this study possible. All the drawings and reconstructions were done by Bruce Cornet.

Evolutionary Theory 7: 231-309 (September, 1986)
The editors thank W. Burger and P.R. Crane for help in evaluating this paper.

Basin of Virginia, and with Recent angiosperms, and is interpreted as a very primitive pre-magnoliid angiosperm close to the evolutionary branch between monocots and dicots. It is concluded that the poor pre-Cretaceous angiosperm record resulted from a combination of factors including poor preservation of delicate organs, the specialized ecology of early angiosperms, large fragile and non-deciduous leaves, and pollen that cannot be easily distinguished from gymnosperm pollen.

* * *

INTRODUCTION

In 1956 Brown described Sanmiguelia lewisii from the Late Triassic Dolores Formation of Colorado, and on the basis of leaf shape and venation, suggested a possible relationship with the Palmae. Subsequently, the phylogenetic relationships of Sanmiguelia have been controversial, and comparisons have been made with taxa ranging from monocotyledons to cycads, and even the probable arthrophyte Schizoneura (Tidwell et al., 1977). With the exception of carbonized leaves reported by Ash (1976), all previously described material of Sanmiguelia consisted of leaf impressions in red siltstone and fine sandstone, or three-dimensional casts of stems with attached leaves (Tidwell et al., 1977).

Since the specimens reported by Ash (1976) came from a previously unrecognized locality in Texas, and had indications of veins preserved between the plications, an attempt was made to recover more complete material from Ash's locality (figure 1). For three days only fragments of leaves similar to those illustrated by Ash were found, but persistence and luck eventually combined to make a story with a happy ending: As the sun began to slip below the horizon on the last planned day of the expedition, one last attempt was made. This time a swing of a pickaxe revealed a nearly complete reproductive axis (Pl. 6, fig. a). With additional excavation in the following months, an entire vegetative colony of Sanmiguelia was discovered in growth position that yielded unusually well-preserved leaves, stems, roots, wood, reproductive axes, seeds, and pollen.

This paper deals primarily with the reproductive organs and leaf venation of Sanmiguelia lewisii. Descriptions and illustrations of wood and root anatomy, additional data on leaf morphology and variation, the wall structure of in situ pollen, and a reconstruction of the entire plant will be published later. Pertinent data on anatomy, however, is briefly discussed and illustrated. All specimens described and illustrated in this paper are deposited in the paleobotanical collections of the Field Museum of Natural History, Chicago (PP).

GEOLOGIC OCCURRENCE

The Sanmiguelia specimens described here come from near the top of the Trujillo Formation of the Dockum Group of northwest Texas (figure 1). Palynoflorules from the matrix containing Sanmiguelia specimens and from nearby shales at the locality are identical to those described by Dunay and Fisher (1979) from the upper Dockum Group, and indicate a Late Carnian age. Dunay and Fisher's (1979) study includes a palynoflorule (7A) from the same

locality. A diverse pollen assemblage was found clinging to some Sanmiguelia leaf cuticles; some of those palynomorphs (e.g. Succinctisporites cf. S. circumdatus Leschik, 1955) are diagnostic of the Carnian (Pl. 2, fig. f). All specimens of Sanmiguelia come from one locality along a dirt road winding down the north wall of Sunday Canyon, just west of Palo Duro Canyon State Park, in Randall County, Texas (Lat. 101° 44'; Long. 34° 50'). The strata containing Sanmiguelia occur just below a sequence of conglomerate and sandstone, and appear to represent a shallowing upwards interdistributary lake deposit on top of a paleosol. The Sanmiguelia colony is restricted to the west end of a long gray mudstone lens, which is terminated westward by a down-cutting sequence of channel sandstone with conglomerate lag at its base (figure 1). The lacustrine clam shrimp, Cyzicus sp., occurs in some of the dark-gray shale interbeds within the lake sequence.

MATERIALS, METHODS, AND OCCURRENCE

The remains of Sanmiguelia lewisii were found both in growth position and as fallen leaf-bearing axes along bedding planes (Pl. 1, fig. a; Pl. 4, fig. a). The vertical axes are preserved as pith casts surrounded either by carbonaceous residue or petrified wood (Pl. 2, figs. a and b). Small plicate leaves are attached to the lower part of some vertical axes (figure 2b), while only sheathing leaf bases are preserved on others (Pl. 2, fig. a) - no large leaves are attached. Most leaves found in the siltstone layers above the paleosol are either twisted, torn, or fragmented, probably reflecting damage during burial.

Portions of large leaves were also found oriented parallel to bedding in the shale directly above the paleosol in which the vertical axes were rooted. Both vertical and fallen (horizontal) axes had attached leaves that are morphologically identical to the leaves of Sanmiguelia lewisii (compare figure 2b with Pl. 1, figs. a-b). Some vertical axes lacking attached leaves (figure 2a) had adjacent fallen axes (e.g. Pl. 1, figs. a-b) possessing Sanmiguelia type leaves, while others had attached leaves only at their distal ends. Although some gymnospermous fossils (isolated leaves, stems, and cones) were found preserved in the paleosol, with few exceptions, Sanmiguelia, its vegetative and reproductive organs, and the remains of ferns were the only determinable fossils found above the paleosol in the sediments surrounding the upright stems.

The friable nature of the sediments presented a problem in removing specimens, which sometimes were larger than the area of the excavation. Damage invariably occurred to some large specimens, with some small pieces of rock crumbling along fractures, joints, and breaks. Several of the specimens have been carefully reconstructed in the laboratory.

Some of the specimens required degaging in order to reveal hidden parts. Most specimens, however, provided enough evidence for study and interpretation without any significant preparation. Acetate peel transfers were made of well-preserved leaves, and a JEOL SEM was used to study individual microsporophylls and transfer preparations of aggregates of microsporophylls from large reproductive structures. Standard palynological techniques were used to secure pollen from microsporangia, as well as

cuticle fragments from megasporophylls. Such preparations of pollen and cuticle, as well as transfer peals of leaf cuticle, were studied and photographed with a Zeiss Photomicroscope with built-in camera. Photographs of the megafossils were made using both Hasselblad 500 cm and Minolta 35 mm cameras with enlargement lenses.

The reproductive organs are not described under Sanmiguelia lewisii, but are given their own binomial names, because 1) two distinctly different types of paniculate inflorescences were found, neither of which was organically connected to Sanmiguelia leaves (even though they overlapped them), 2) it is preferable that each inflorescence type have its own designated holotype and a formal diagnosis and description, 3) a taxon based on leaves suffers the risk of becoming a formgenus if the morphology of its leaves proves to be generalized within a natural genus or family, 4) the leaves at the Sunday Canyon locality, although they are indistinguishable in general form from S. lewisii, may belong to a different species, and 5) later investigators can always place these names in synonymy with S. lewisii or designate one or more of the names as taxa distinct from S. lewisii. The dispersed seeds are given a separate name even though identical seeds were found inside a mature megasporophyll, because dispersed pollen is given a separate name even when its origin is known. A third type of reproductive structure resembling a part of one of the paniculate inflorescences was found attached to stems bearing Sanmiguelia leaves, but this third type is interpreted here only as supporting evidence that the paniculate inflorescences belong to Sanmiguelia.

SYSTEMATIC DESCRIPTIONS

Sanmiguelia Brown **emend. gen.**

TYPE SPECIES: Sanmiguelia lewisii Brown

EMENDED DIAGNOSIS: Primary axis or stem simple, round in transverse section, erect. Narrow elongate secondary branches originate at low angles from primary axis and diverge outwards. Small to large leaves borne singly on primary axis in a loose to crowded spiral. Very small leaves and bracts borne singly on secondary axis in a loose spiral. Leaves broadly oval or elliptic in shape, widest in the middle, tapering to an acute or acuminate apex (tip frequently missing); narrow below, but not petiolate and attached by a broad transverse base, which clasps and decurrently sheathes the stem.

Leaves with up to four orders of parallel venation. All vein orders anastomose and bifurcate: Primary veins rarely, secondary veins occasionally, tertiary veins commonly, and quaternary veins abundantly. Tertiary and quaternary veins often

****

Figure 1. Index map of part of the southwestern United States and a stratigraphic section of the rocks exposed in the Sunday Canyon branch of Palo Duro Canyon, Texas. The approximate position of the locality containing Sanmiguelia leaves and reproductive remains in Sunday Canyon is indicated on the section (modified after Ash, 1976, Text-fig. 1).

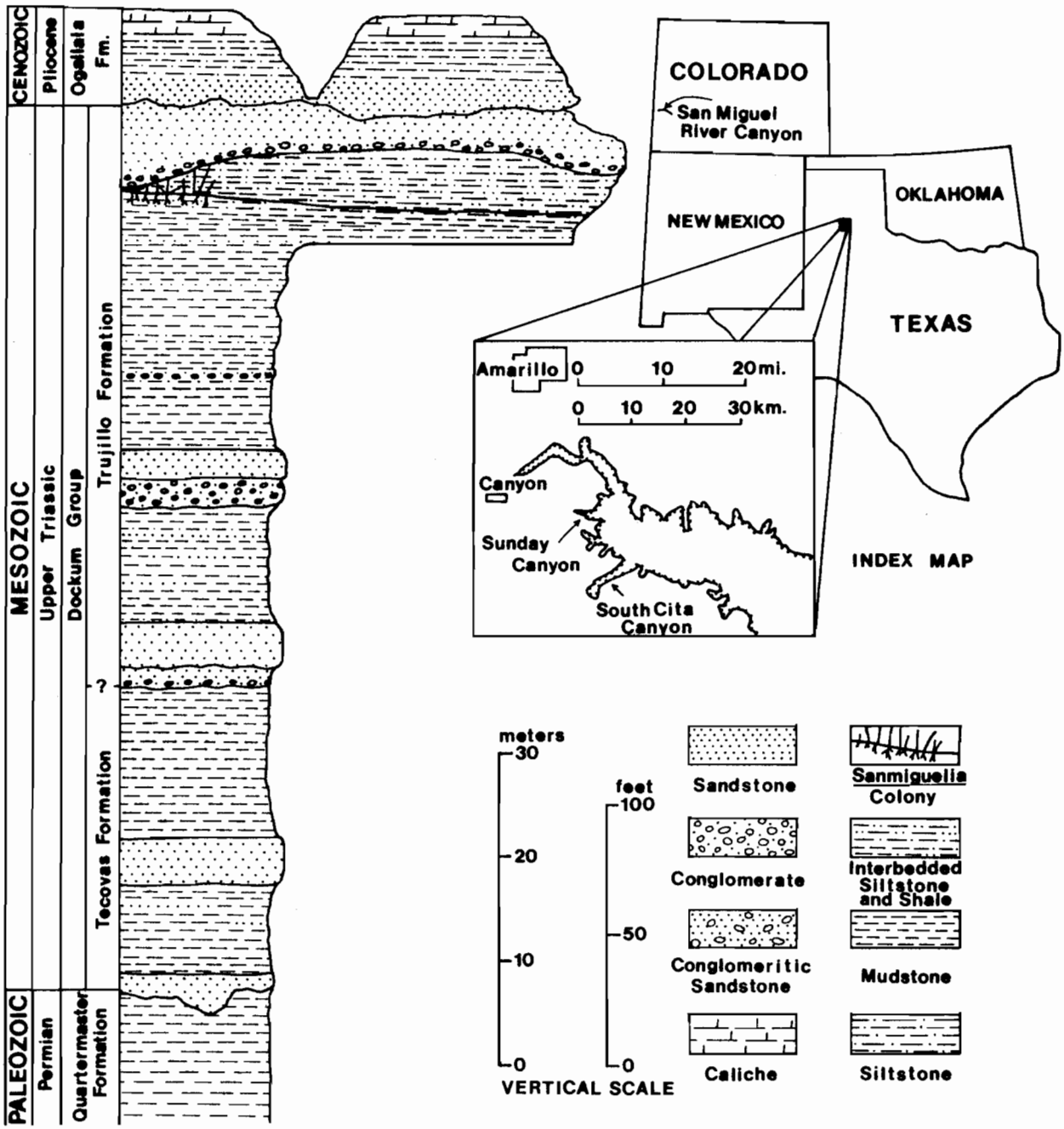
CENOZOIC
Pliocene
Ogallala Fm.
MESOZOIC
Upper Triassic
Dockum Group
Trujillo Formation
?
Tecovas Formation
PALEOZOIC
Permian
Quartermaster Formation
COLORADO
San Miguel River Canyon
NEW MEXICO
OKLAHOMA
TEXAS
Amarillo
0 10 20mi.
0 10 20 30km.
Canyon
Sunday Canyon
South Cita Canyon
INDEX MAP
meters
30
20
10
0
feet
100
50
0
VERTICAL SCALE
Sandstone
Conglomerate
Conglomeritic Sandstone
Caliche
Sanmiguelia Colony
Interbedded Siltstone and Shale
Mudstone
Siltstone

forming distinct cross veins. Leaf surface strongly marked by numerous longitudinal plications running parallel to veins from base to apex. Quaternary and tertiary veins fusing in the leaf apex to form larger veins as vein density increases. Cross veins interconnect reformed "secondaries" (based on width only) in apex as smaller veins disappear. Primary veins broad and massive, restricted to base of leaf and sheathing leaf base. More persistent primaries as well as secondaries frequently occupying folds in plications. Tertiary and quaternary veins emerge from and anastomose with vein of origin to form elongate narrow loops, unite with adjacent vein immediately after emerging or after forming a long parallel vein, or cross one or more veins before uniting with a vein of equal or lower rank. Small leaves tend to have fewer vein orders, with very small apical leaves or bracts having one large central vein and a pair of small marginal veins.

Sanmiguelia lewisii Brown **emend. sp.**

LECTOTYPE: USNM 167538.
HYPOTYPE: BYU 1512, 1584, 1585.

REFERENCES: 1956 Sanmiguelia lewisii Brown, U.S. Geol. Surv. Prof. Pap. 274H, p. 205-209, Pl.32, figs. 1-2; Pl. 33, fig. 2.
1961 Sanmiguelia lewisii, Andrews, p. 172, fig. 6-1.
1962 Paloreodoxites lewisii (Brown) Bock, Geol. Cent. Res. Series, V. 2, p. 283-285, fig. 504.
1963 Sanmiguelia lewisii, Arnold, Col. J. Ind. Bot. Soc., V. 42A, p. 4-9, Pl. 1, fig. 1.
1964 Sanmiguelia lewisii, Becker, Gard. Journ. p. 231-233.
1969 Paloreodoxites lewisii (Brown) Bock, Geol. Cent. Res. Series, V. 3, p. 242-254, figs. 402, 403, 407.
1972 Sanmiguelia lewisii, Becker, Palaeontogr., V. 138B, p. 181-185, Pl. 38, figs. 3-4.
1976 Sanmiguelia lewisii, Ash, J. Paleont., V. 50, p. 799-804, text-fig. 2.
1976 Sanmiguelia lewisii, Hughes, Palaeobiology of Angiosperm Origins, Cambridge Univ. Press, p. 175-179, fig. 13.1, Table 13.1.
1977 Sanmiguelia lewisii, Tidwell et al., Palaeontogr. V. 163B, p. 143-151, Pl. 1, figs. 1-2, 4; Pl. 2, figs. 2-6; Pl. 3, fig. 4; text-fig. 4.

NEW MATERIAL: PP34337-PP34343, PP34345-PP34358, PP34410-PP34416: stems, roots, rhizomes; PP34344, PP34359-PP34409: leaves.

NUMBER OF SPECIMENS EXAMINED: 80 (leaves and stems in organic connection above paleosol counted as one specimen).

ILLUSTRATIONS: Pl. 1, figs. a-h; Pl. 2, figs. a-k; Pl. 3, figs. g-i; Pl. 4, fig. i; Pl. 7, figs. m-n; Pl. 8, figs. a, d-i; figures 2-4.

EMENDED DIAGNOSIS: As for the genus. Erect plant, at least 65 cm in height. Each primary axis or stem usually with its own

downwardly dividing root stock. Plant typically in vegetative clusters of two or three stems spaced 25 cm to 45 cm apart and connected by subsoil rhizomes. Some stems of a vegetative colony lacking a root system, arising directly from a rhizome. Occasionally two stems originated from the same root stock, and additional stems arose to replace those broken off near their bases. Satellite plants, spaced 85 cm to 175 cm from vegetative clusters, connected to an underground rhizome system.

Leaves spirally arranged around a stem 3-4 cm in diameter. Stems consisting of a large central pith 10-18 mm in diameter surrounded by a woody cylinder, which developed in the lower part of the stem outside a ring of primary vascular bundles, and is broadest at the base of the plant. Lower and upper leaves of mature plant reached 30 cm in length by 19 cm in width with 10-12 plications. Middle leaves reached 48-60 cm in length by 28-31 cm in width with 24 plications. Leaves smaller near base of plant, decreasing in length down to 5 cm with 10 plications. Sheathing leaf bases up to 7 cm long. Leaves of secondary branches much smaller, decreasing to cataphylls 1 cm or less in length at ends of branch. Secondary branches arising between sheathing leaf bases and stem, but not demonstrably in the axils of leaves. Secondary branches capable of assuming upright growth and continuation of primary axis if main stem broken.

Medium to large leaves with four orders of venation, parallel to the plications. Vein orders defined by width: Primary veins 1.0 mm-2.5 mm in width, forming 4 mm-11 mm wide longitudinal strips of lamina containing recognizable anastomosing and bifurcating vascular bundles. Primary veins separated mainly by tertiary and quaternary veins, with secondary veins arising from division of primaries. Secondary veins 0.4 mm-0.99 mm in width. Tertiary veins 0.1 mm-0.39 mm in width. Quaternary veins less than 0.1 mm in width down to single strand of tracheids. Primary, secondary, and tertiary veins composed mainly of scalariform tracheids; tertiary and quaternary veins composed of scalariform or reticulate tracheids; quaternary veins sometimes composed of single or double strands of annular-helical tracheids. Larger veins sometimes with associated resin cells and elongate bodies of resin. Cross veins joined all orders of parallel veins, occurred within bundles of larger veins, and formed loops and interconnections that resemble an imperfect reticulum. A small vein of tertiary rank followed margins of leaf, and was joined by crossing tertiary and quaternary veins. Stomata abundant and possibly actinocytic, tending to be oriented perpendicular to parallel veins. Stomata tending to be oriented parallel to veins between some closely-spaced veins. Epidermis thin, moderately covered with single hairs and dendroid trichomes.

DESCRIPTION: Sanmiguelia lewisii evidently exhibited vegetative reproduction in which clusters of vertical stems arose from underground rhizomes (figure 2). Branching root systems extended downwards at least 8 cm below the top of the paleosol, with two or three major divisions of the primary root occurring within the top 4 cm of the paleosol. Traces of small roots ocurred as far down as 15-20 cm below the top of the paleosol, but due to their variable paths through the friable clayey siltstone, organic connection with the roots of Sanmiguelia could not be

verified. Some siderite petrifactions of primary roots (Pl. 8, fig. a) yielded excellent preservation, showing a subrounded (terete) woody stele, possible cambium, scattered vessels, and tracheids possessing crowded simple pits and scalariform end plates (Pl. 2, figs. c-e).

Although the differences in preservation between the Colorado and Texas localities precluded a direct comparison of leaf shape and size along the stems (most, but not all, of the leaves along the stems at Sunday Canyon were missing, and the stems had collapsed around sediment-filled pith casts), leaves were found in the shaley sediments on top of the paleosol. Some of those were attached to fallen stems (Pl. 1, figs. a and b; Pl. 5, figs. a, b, and f). All the leaves, fallen or attached to upright stems, fit the criteria of Sanmiguelia based on descriptions and illustrations of leaf impressions (cf. Tidwell et al., 1977). The added similarity of growth habit and size for the entire plant permits the identification of the Sunday Canyon fossils as S. lewisii.

The form, size, and disposition of the leaves on the main axis are adequately described by Tidwell et al. (1977), and need not be repeated here. The venation, epidermis, and stomata, however, are preserved in the new material, and are described below:

The leaves of Sanmiguelia lewisii possess four orders of parallel veins. These orders are based on width (see diagnosis), since veins of higher rank diverge at low angles from veins of lower rank, and arise from them either laterally or by unequal division or dichotomy (Pl. 1, fig. h; figures 3g and 3h). All but the smallest veins were observed to divide, and most types of veins, with the exception of primaries, were observed to anastomose with veins of equal or lower rank. Some veins were observed to end blindly, although this was attributed to damage during preservation or preparation. Primary veins are restricted to the base of the leaf (Pl. 2, fig. h), where they arise from an elongate sheathing leaf base containing numerous closely-spaced wide veins. As the primary veins divide upwards in the basal part of the leaf blade, they form bundles of smaller primaries separated mostly by tertiary and quaternary veins. Secondary veins are the direct continuation of primary veins as their thickness is reduced through division. Secondary veins rarely form cross veins, and either arise through the upwards division of primaries (Pl. 1, figs. g and h), or reform in the leaf apex through anastomosis (Pl. 3, fig. f; figure 3i).

Tertiary and quaternary veins comprise the bulk of the veins in any portion of the leaf, except its base. Whereas primary and secondary veins tend to occupy the folds in the plications, the tertiary and quaternary veins span across the plications (Pl. 1, fig. c). Tertiary veins occasionally form cross veins (Pl. 2, fig. k), but usually parallel other veins until they drift toward a vein and fuse with it (Pl. 2, fig. j). Such fusion is usually only temporary, since the resulting vein eventually divides (except in the leaf apex). Quaternary veins, by contrast, are more versatile, since they form parallel veins, vein loops, and cross veins (Pl. 2, fig. j; figures 3g and 3h). Quaternary veins are also the most diverse in terms of composition of their vascular tissue, which consists of annular-helical (Pl. 1, fig. e),

scalariform (Pl. 2, figs. g and j; Pl. 3, fig. h), and reticulate (Pl. 7, fig. m) tracheids.

Whereas leaf impressions from Colorado do not preserve any evidence for cross veins, transfer preparations of leaves from Texas show abundant evidence for them (Pl. 1, fig. h; Pl. 2, figs. g and j; Pl. 3, figs. h and i; figures. 3g, 3h, and 3i). Cross veins are typically less than 0.1 mm wide, and most are similar in width to quaternary veins. Occasionally, quaternary veins can turn into cross veins as they deviate from their previously parallel course and join an adjacent vein (Pl. 2, fig. j). Cross veins either join adjacent veins directly (Pl. 1, fig. h, at arrows; Pl. 3, fig. h; figures 3g and 3h), or cross one or more veins before rejoining a vein (Pl. 3, fig. i; figure 3g). Veins that naturally cross others were distinguishable from the occasional vein that was displaced or distorted during preservation, because both ends were observed to join other veins. Cross veins even form loops, crossing one vein more than once (Pl. 3, fig. i; figure 3g). Cross veins can be found within the lamina of the leaf between plications, between closely spaced veins in the folds of plications, and between the crowded veins in the leaf apex. Cross veins are typically composed of scalariform tracheids (Pl. 3, fig. h), but like quaternary veins, can contain reticulate or annular-helical tracheids.

Measuring the density and percentage of each vein type gives an indication of changing vein morphology from the base to the apex of a leaf (summarized in Table I):

Two leaf fragments measuring 17 mm and 13 mm wide from near the base of a large leaf have vein densities of 1.76/mm and 1.82/mm, respectively. The narrower leaf fragment has one primary (3%), six secondaries (20%), 10 tertiaries (33%), and 13 quaternaries (44%) (Pl. 2, fig. h). The wider leaf fragment has two primaries (6%), three secondaries (10%), 11 tertiaries (35%), and 15 quaternaries (49%).

A large folded leaf fragment measuring 140 mm wide has a vein density of 2.4/mm across the middle 80 mm wide surface exposed on one side of the specimen (Pl. 1, fig. c). The tapering margins and size of this fragment indicate it came from the upper middle of a nearly mature leaf. A significant shift toward smaller veins has occurred, with an absence of primaries, 11 secondaries (6%), 63 tertiaries (32%), and 121 quaternaries (62%).

The percentages of vein types in the leaf apex resembles that near the base of the leaf, with the exclusion of primaries (Table I). A large portion of one apex (Pl. 3, fig. f; figure 3i) may represent a leaf that is not fully enlarged, because it tapers more gradually than the apices of large leaves illustrated by Tidwell et al. (1977). The lower part of this fragment is 37 mm wide, and has a vein density of 2.2/mm. The density increases in the 10 mm wide leaf tip to 3.4/mm. Primary veins are absent, while secondaries increase from two (2%) to nine (27%) going into the tip. Tertiaries decrease from 36 (44%) to 11 (32%), and quaternaries decrease from 45 (54%) to 14 (41%).

By contrast to the above leaf fragments, which could all have come from leaves of similar size, another leaf fragment (Pl. 3, fig. i) shows a significant increase in quaternary veins. This 30 mm wide fragment may represent the widest portion of the lamina in the upper part of a fully expanded mature leaf. Vein

density is 2.9/mm. There are only two secondaries (2%), 10 tertiaries (12%), and 75 quaternaries (86%), many of which nearly reach the lower width limit (0.1 mm) for tertiary veins (figures 3g and 3h).

A 22 mm wide fragment from the lower half of a smaller leaf demonstrates how quaternary veins could have increased through the lateral division of tertiary veins in a leaf expanding by means of an intercalary meristem. Vein density is 2.1/mm, which is intermediate between values for the base and middle of a leaf. There are only four secondaries (8%), 31 tertiaries (66%), and 12 quaternaries (26%).

TABLE I

Portion of Leaf:	BASE	LOWER	MIDDLE	UPPER	TIP
Vein Density: per mm width	1.76-1.82	2.1*	2.4	2.2-2.9	3.4
Quaternaries:	44-49%	26%	62%	54-86%	41%
Tertiaries:	33-35%	66%	32%	44-12%	32%
Secondaries:	20-10%	8%	6%	2%	27%
Primaries:	3-6%	-0-	-0-	-0-	-0-

* Possibly from a smaller less mature leaf.

****

Some of the larger veins, particularly those along the folds of plications, occasionally have elongate narrow bodies of resin associated with them (Pl. 1, figs. c at arrows and d; Pl. 3, fig. i at arrows). High magnification shows these bodies to be composed of small beads of resin (1.5-20 um in diam.), which either parallel or overlie a vein between the cuticles, and follow the veins for distances up to 2.5 cm (Pl. 1, fig. d; Pl. 2, fig. i).

Leaf cuticles are thin, and cell outlines are difficult to observe, perhaps due to the superposition of upper and lower cuticles (Pl. 3, fig. g; Pl. 7, fig. m). Most epidermal cells appear to be very small (on the order of 8-14 um long). Between closely-spaced veins, particularly in the lower part of the leaf, cells are longer and occur in files parallel to veins (Pl. 1, fig. d; Pl. 3, fig. h). Epidermal cell shape is more isodiametric and variable, however, over most of the cuticle, particu-

****

Figure 2. Sanmiguelia lewisii Brown, preserved at the Sunday Canyon locality as sediment-filled pith casts, which terminate at various levels (S1-S4) within shallow lacustrine and overbank deposits, and which are rooted in a paleosol (P) underlying the entombing silt-dominated sediments. Note small plicate leaves and leaf bases attached to some axes, dark gray shale overlying paleosol (shaded pattern), subsoil rhizomes interconnecting the axes, and branching roots within the paleosol. Changing widths of stems are given in mm and the distribution of secondary xylem is indicated by a basally increasing gap between stem and pith cast diameters.

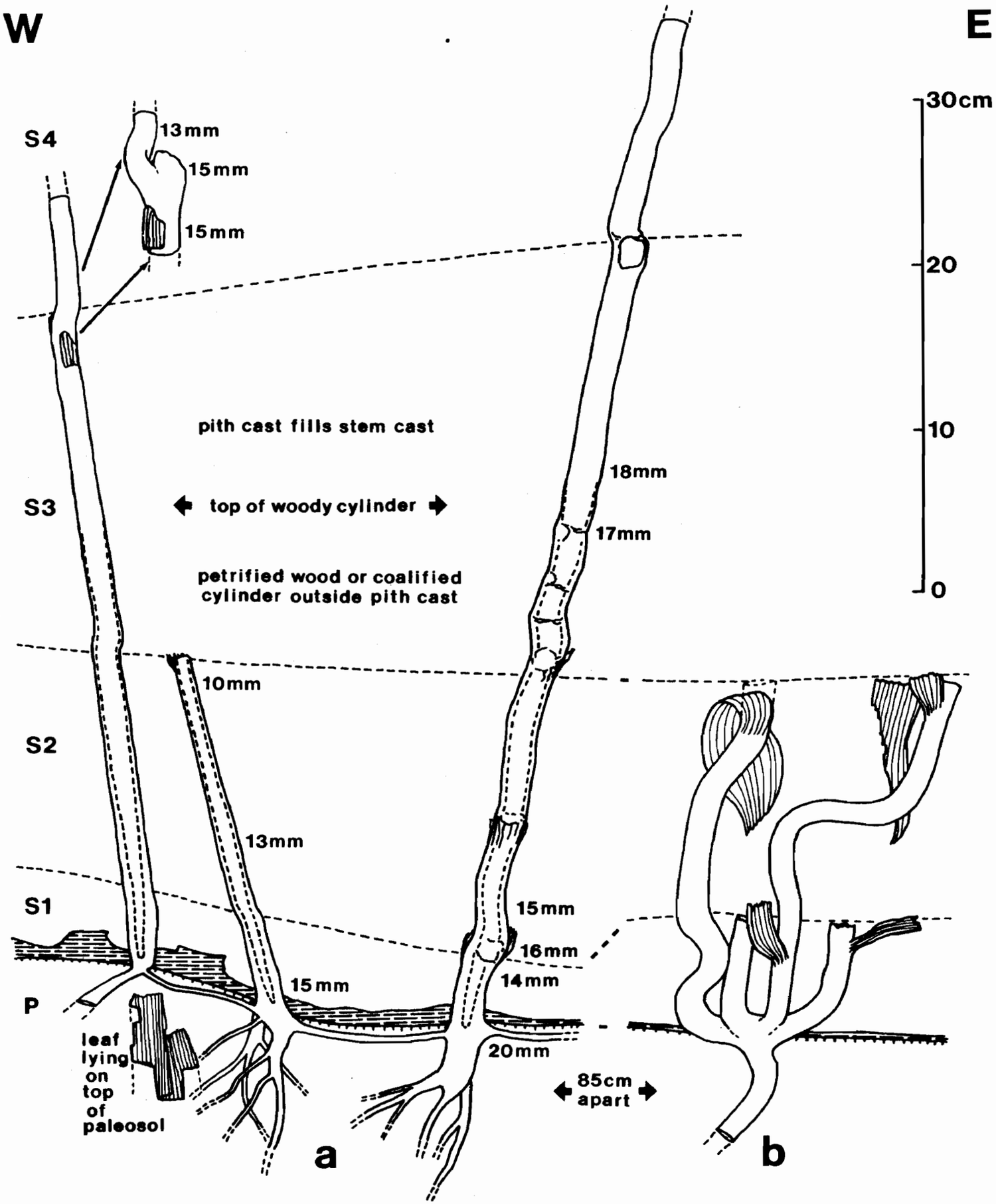
W
E
30cm
20
10
0
S4
S3
S2
S1
P
13mm
15mm
15mm
pith cast fills stem cast
top of woody cylinder
petrified wood or coalified cylinder outside pith cast
18mm
17mm
10mm
13mm
15mm
16mm
14mm
15mm
20mm
leaf lying on top of paleosol
85cm apart
a
b

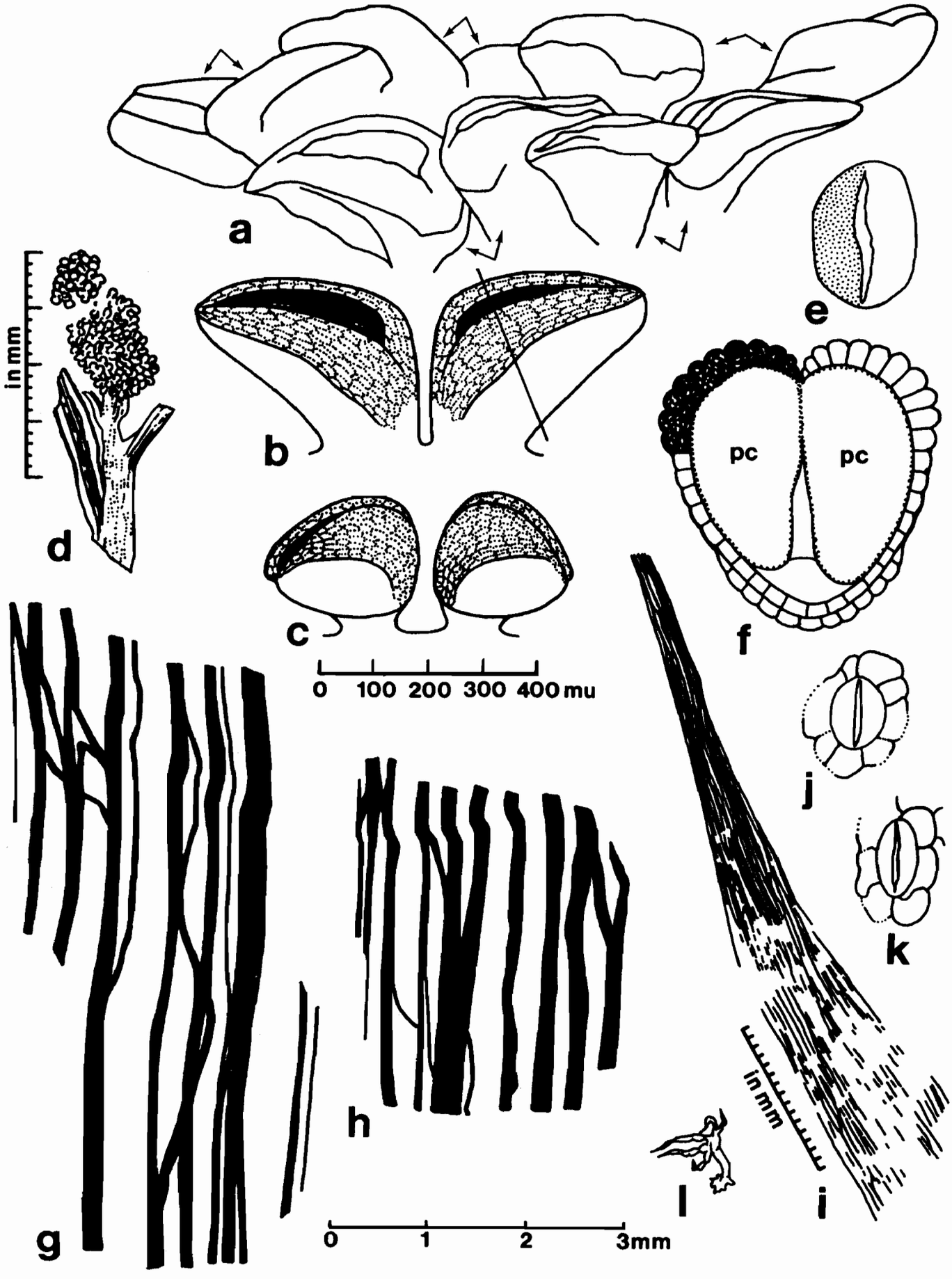
a
b
c
d
e
f
pc
pc
g
h
i
j
k
l
in mm
in mm
0 100 200 300 400 mu
0 1 2 3mm

Apical venation resembles leaf-base venation (Table I), and primary and secondary veins are typically composed of bundles of smaller veins (Pl. 2, fig. h), suggesting that mesophyll initials were intercalated between bundles of procambial initials. As the leaf lamina widened during its initial stages of growth, smaller veins emerged by the development of mesophyll initials between differentiating closely-spaced procambial bundles. If mesophyll initials did not proliferate, a wide vein formed like that found in the clasping leaf base and in small apical leaves on determinate secondary branches (Pl. 5, fig. d). As mesophyll tissue differentiated between developing vascular bundles, the direction of primary growth was lateral, rather than apical. Lateral growth resulted in the orientation of guard cell pairs parallel to the direction of growth, or perpendicular to the veins (Pl. 2, fig. g; Pl. 7, fig. m). The orientation of guard cells is direct evidence for intercalary growth and plate meristems between parallel veins in Sanmiguelia leaves. Maturation appears to have progressed basipetally from the narrow apex to the widest portion of the leaf, then decreased towards the leaf base. Only between closely spaced veins that experienced minimal lateral growth (mainly near or at the base of the leaf) are stomata and epidermal cells oriented predominantly parallel to the veins.

POLLEN-BEARING REPRODUCTIVE STRUCTURES OF SANMIGUELIA

Synangispadixis Cornet gen. nov.

TYPE SPECIES: Synangispadixis tidwellii Cornet sp. nov.

DIAGNOSIS: Reproductive axis without apparent bracts or leaves, tapering apically, bearing hundreds of helically arranged secondary axes; main axis wide at base, long, flexible. Secondary axes covered with hundreds of sessile, biloculate, double-walled microsporophylls, each with a constricted base. Microsporophylls arranged in opposite pairs. Microsporophyll pairs arranged in a tight spiral around immature secondary axes. Secondary axes along basal part of main axis elongate, wide ("fleshy" or expanded), with loosely-arranged dehisced microsporophylls. Secondary axes higher on main axis progressively shorter, narrower, with undehisced microsporophylls containing immature pollen. At apex secondary axes bear smaller immature microsporophylls. Microsporophylls elliptical to elongate, having an adaxial outer wall of thickened endothecial or "fiber" cells, an epidermal cuticle along constricted microsporophyll base, and a longitudinal adaxial slit over a septum separating two pollen masses. Each pollen mass surrounded by the remnants of a tapetum. Septum largely disappears at maturity, producing one united pollen chamber containing hundreds of small, elliptical, psilate tectate-granular monosulcate pollen.

DERIVATION: From syn - Greek, meaning together, with, united; angio - Greek, meaning vessel or container of any kind, capsule, seedcase (or sporecase) of plants; spadix - Greek, meaning a spike of flowers on a fleshy axis, whether perfect or imperfect, naked or with perianth; also synangia - plant structures with united microsporangia.

DISCUSSION: This genus is established for the large male reproductive axes associated with Sanmiguelia, and which probably terminated the main axis of Sanmiguelia lewisii. The secondary "fleshy" branches covered with crowded sessile microsporophylls closely resemble synangia borne along the spadix of some aroids. The condensation of microsporophylls on specialized branches is interpreted as a type of synangia, even though the microsporophylls are not joined to each other. The enlargement of the secondary axes at the time of pollen dehiscence is comparable to the enlargement of aroid spadices during anthesis.

Pollen-bearing structures identical to the secondary branches of Synangispadixis terminate some secondary vegetative branches of Sanmiguelia. They are borne individually or in clusters of up to three, suggesting that the secondary branches of Synangispadixis are specialized organs (i.e. synangia) and not just branches bearing microsporophylls. The organic connection of these organs to Sanmiguelia supports the interpretation that Synangispadixis belongs to Sanmiguelia, but since Synangispadixis was not found in organic connection with Sanmiguelia and it represents a distinctive reproductive structure, it is given its own name. Should Synangispadixis and Sanmiguelia be found in organic connection, the name taking priority will depend on the systematic treatment of the leaves.

Synangispadixis tidwellii Cornet **sp. nov.**

HOLOTYPE: PP34322.
HYPOTYPE: PP34323.

DIAGNOSIS: As for the genus.

REFERENCES: `unknown cone' adjacent to `Paloreodoxites lewisii', Bock (1969: 245, fig. 405, photograph & line drawing).

OTHER MATERIAL: PP34326-PP34327.

RELATED MATERIAL: PP34324-PP34325, PP34328.

NUMBER OF SPECIMENS EXAMINED: 7.

ILLUSTRATIONS: Pl. 3, figs. a-e; Pl. 4, figs. a-h; Pl. 5, figs. a-e, g; Pl. 7, figs. a-b; figure 8b.

DERIVATION: After William D. Tidwell, Professor of Botany, Brigham Young University, for his paleobotanical contributions to our understanding of Sanmiguelia and his courage in publishing controversial evidence in support of pre-Cretaceous angiosperms.

DESCRIPTION: One virtually complete reproductive axis (Pl. 3, fig. a), the distal portion of a second (Pl. 4, fig. a), and a mature portion of a third (Pl. 3, fig. b) were found intimately associated with Sanmiguelia leaves and stems. These reproductive structures appear to have been borne terminally on the main axis for three reasons: 1) the width and size of their central axis compares with that of the distal portions of Sanmiguelia primary axes; 2) the paniculate branch system lacks bracts or leaves, and

is naked for its entire preserved length, which is unlike the leaf-bearing secondary branches of Sanmiguelia that terminate in pollen-bearing organs; and 3) one specimen shows the distal portion of an axis overlying one(?) frayed or ripped Sanmiguelia leaf. The orientation of these specimens is such that they may have been attached (Pl. 4, fig. a; see also figure 8b for an interpretation).

The main axis of the complete reproductive axis (Pl. 3, fig. a) is 24.2 cm long, 14 mm wide at its base, and contains numerous individual vascular strands, which appear to anastomose and bifurcate along the axis. SEMGs of these vascular strands show mostly helical-scalariform tracheids (Pl. 3, fig. a'; also Pl. 1, fig. f). The main axis is naked and branchless for the basal 4 cm, tapers gradually to 8 mm in width where the secondary axes begin, and continues with that width for about 6 cm, or until the secondary axes decrease in length (Pl. 3, fig. a, arrow). The main axis abruptly decreases to 5 mm (at arrow), and thereafter gradually decreases to less than 2.5 mm in width near the apex.

The proximal secondary axes are 18-19 mm in length; this length is maintained for 6 cm along the main axis. Above that point on the main axis the secondaries abruptly decrease in length to 11 mm (Pl. 3, fig. a, arrow). Subsequently, the secondary axes gradually decrease in length apically from 11 mm to about 6 mm. They are spirally attached along the main axis, but due to compression and burial, only the lateral branches can be clearly seen. There are about 40 elongated secondary axes visible along the basal 6 cm, and about 60 secondaries over an 8 cm length of main axis distally. An estimated 80 secondaries surrounded the basal 6 cm of main axis, with over 280 secondaries apically. The elongation and increase in width of the proximal secondaries coincides with maturity, since most of the microsporophylls on those branches have dehisced, while the pollen sacs of microsporophylls on the shorter and narrower distal secondaries (above arrow in Pl. 3, fig. a) are still full.

The secondary axes depart from the main axis at right angles, and, except for the basal 1-3 mm, are entirely covered with sessile biloculate microsporophylls. These secondary axes are interpreted as synangia, even though the microsporophylls are not fused to each other, because very similar structures were found terminating vegetative secondary branches of Sanmiguelia, either individually or in clusters of three or more(?) (Pl. 5, figs. a-d; figure 3d). The similarity of pollen-producing structures suggests that the secondary branches of Synangispadixis are specialized organs that were genetic units, and resulted from the fusion or coalescence of numerous microsporophylls as in a synangium. The vegetative branches of S. lewisii that terminate in reproductive organs have small parallel-veined cataphylls that decrease in size apically. As these cataphylls decrease in size, their venation condenses to a wide central vein flanked by a pair of marginal veins (Pl. 5, fig. d). No cataphylls, bracts, or leaf-like organs were observed on Synangispadixis.

The microsporophylls are bilaterally symmetrical, longer than wide, and basally constricted where they join the secondary axis. Laterally they range in shape from lunate to tear-drop (Pl. 3, fig. c; Pl. 4, fig. f-h; Pl. 5, fig. g; figure 3a-3c). They range in length from 230 to 525 um, and in height from 170

to 351 um. Most are longer than tall (e.g. 330 um by 240 um), while others are taller than long (e.g. 280 um by 351 um). A longitudinal suture runs adaxially across the apex and down the ventral side, and is distally flanked by large rectilinear cells with their short axes typically oriented perpendicular to the suture (Pl. 3, fig. c; Pl. 4, figs. e-g). These cells are much larger adjacent to the suture than along the sides of the microsporophylls, and form a protruding ridge on both sides of the suture (Pl. 3, fig. c; Pl. 4, figs. g-h; Pl. 5, fig. g). The cells within the ridges appear to contain an internal structure consisting of fiber-like thickenings of the cell walls (Pl. 7, fig. b; figure 4a), while much smaller cells below the protruding ridges contain an internal structure consisting of fused granules (Pl. 4, fig. e). The enlarged cells may be a structural adaptation for the opening of the anther sac. Their external position could be interpreted as indicating an epidermal origin, but their morphology is more comparable to the fibrous endothecial cells of angiosperm anthers, which frequently occupy an external position (an epidermal cell layer disappears early during ontogeny: Eames, 1961). Sometimes remnants of a waxy cuticle are preserved as scabs or beads upon the enlarged cells bordering the suture (Pl. 4, fig. b'). The lower part or base of each microsporophyll appears to be covered by an epidermis (figure 3f), which extends upwards from the axis, forming a wrinkled layer covering an inner endothecial layer (figures 4b-4c, ep; Pl. 3, fig. c; Pl. 4, fig. h). Between the thickened cells forming the ridges bordering the suture and the upper limits of the epidermis, the endothecial layer forms the major part of the wall (figure 3f), and there it commonly shows signs of damage (Pl. 3, fig. c; Pl. 4, fig. h).

The microsporophylls are tightly packed and appear to be spirally arranged along immature secondary axes (Pl. 5, fig. c), but are loosely packed on expanded mature axes (Pl. 3, fig. b; Pl. 5, fig. g). They are borne back to back in pairs on the secondary branches (Pl. 4, fig. f; Pl. 5, fig. g; figures 3a-c), and the sutures of adjacent microsporophylls are opposite one another. The apices of the microsporophylls are frequently pointed (Pl. 4, fig. b; Pl. 5, fig. g; figure 3a), but may also be blunt or rounded (Pl. 4, figs. g, h).

Many microsporophylls contain pollen preserved in two distinct masses, separated by a noticeable septum (Pl. 7, figs. a, b; figures 4a-4c), while others contain only a single mass (Pl. 4, figs. b-c). Of the five specimens broken open and observed under SEM, four possess a septum between two masses of pollen (figures 4a-4c). The septum is massive and amorphous in cross section (Pl. 7, fig. b, se; figures 4a-4c), while outer wall layers commonly show remnants of cellular structure, suggesting that the septum formed from the coalification of cells with thin or weak cell walls. The septum also appears to vary in thickness and extent of development (compare figures 4a-4c). Individual microsporophylls were oxidized and cleared in NaOH in order to determine the number of pollen "sacs". Most of them (presumably the less mature ones) yielded two pollen masses, sometimes with remnants of a septum still attached (Pl. 7, fig. a). A few yielded a single, large bilobed pollen mass with either a long narrow cleft (Pl. 4, figs. b-c) or a broad deep cleft (Pl. 5, fig. e) separating the two lobes. After

dehiscence, only one pollen chamber is visible within each microsporophyll (Pl. 4, fig. f; Pl. 5, fig. g).

Pairs of yellow-orange pollen masses isolated from a single microsporophyll frequently are of unequal size (cf. Pl. 7, fig. b; figures 4a-4c). Isolated masses are compressed and range in size from 285 um to 380 um in length. SEMGs of their surfaces show pollen covered by sporopollenin-coated (acid-resistant) cellular debris and Übish bodies (Pl. 4, figs. c, d). Only the vague outlines of pollen can be seen through this pollen sac wall and tapetal debris (Pl. 4, fig. c; Pl. 5, fig. e). The pollen is small, elliptical, tectate-granular, and monosulcate, but the sulcus is poorly defined and irregular in shape (Pl. 3, figs. e, d; Pl. 4, fig. d; figure 3e). Pollen from mature microsporophylls (e.g. just above arrow in Pl. 3, fig. a) can be partially disaggregated through maceration, while that from immature ones cannot. Mature (oxidized) pollen ranges in length from 21 um to 29 um (median 24 um), and in width from 11 um to 19 um (median 15 um). Unoxidized pollen is about half that size (Pl. 4, fig. d). A granular infrastructure can be viewed in transmitted light (Pl. 3, figs. e, d). Internal granae are visible where the tectum either has not completely formed on immature pollen or has been removed (Pl. 4, fig. d). The absence of any internal structure in dispersed pollen of identical overall morphology (from the rock matrix of specimens) suggests that mature Synangispadixis pollen may have lacked any distinctive characteristics which might distinguish it from monosulcate gymnospermous pollen.

DISCUSSION: Synangispadixis tidwellii **sp. nov.** appears to have matured acropetally over a long period of time (i.e. days or even weeks). Its unisexual condition and long flexible central axis suggest that it was morphologically adapted for wind pollination, but the inflorescence was probably enclosed by a spathe or large protective leaf early in its development, thereby shielding the proximal secondary branches as they reached anthesis (cf. figure 8). Entomophily may have been important during early development, while anemophily may have predominated later when the spathe-like leaf opened up or the inflorescence grew higher than the leaf.

Each microsporophyll had two pollen masses containing an estimated 300 pollen grains each. If each secondary branch bore an estimated 400 microsporophylls (about 200 counted per side), and four branches encircling the main axis matured at one time, about 960,000 pollen grains would have been released at each successive stage of anthesis. A reproductive axis like the holotype (Pl. 3, fig. a) possessed a minimum of 360 secondary branches, and would have released over 345 million pollen grains as it matured. The relative scarcity of simple monosulcate pollen in the sediment or clinging to the cuticles of the leaves (most of the other pollen types in the sediments are found on the leaves) suggests either that Synangispadixis effectively dispersed pollen through the wind to distant localities, or that insects played a role in selectively removing and transporting pollen without much of it falling into the surrounding sediments.

The presence of two distinct pollen masses, which are separated by a septum that disappears with maturity, gives the microsporophylls a morphology and ontogeny like that of angio-

sperm anthers. The tapetal debris and Ubish bodies surrounding each pollen mass (Pl. 4, figs. c-d), but not present within it (cf. Pl. 3, fig. d), suggest that the tapetum may have been secretory rather than ameboid in function (see Eames, 1961, p. 142). The overall shape, sessile nature, and the extension of a suture most of the way down one (ventral) side of the microsporophyll (Pl. 4, fig. g) give it a primitive carpel-like shape (see figure 10 for comparison). The importance of this resemblance will be discussed under evolutionary significance below.

The occurrence of secondary vegetative branches ending with one or more synangia-like side branches of Synangispadixis suggests that the large reproductive axis was borne at the end of a stem that became progressively more fertile with successive vegetative branches (see figure 8 for a reconstruction). Whether a rhizomatous vegetative colony of three or more closely-spaced stems was monoecious or dioecious is not known for certain, but ovule-bearing and pollen-bearing reproductive branch systems were found lying very near one another adjacent to vegetative colony A in figure 2.

OVULE-BEARING REPRODUCTIVE STRUCTURES OF SANMIGUELIA

Axelrodia Cornet **gen. nov.**

TYPE SPECIES: Axelrodia burgeri Cornet **sp. nov.**

DIAGNOSIS: Long indeterminate primary reproductive axis probably terminating vegetative axis. Main axis unbranched proximally, with at least two orders of branching distally, bearing spirally-arranged, widely-spaced, small parallel-veined clasping bracts on lower half, and long pointed parallel-veined bracts or cataphylls with elongate sheathing bases on upper half. Cataphylls increase in length distally up to first secondary branch, become closely-spaced with overlapping sheathing bases, then decrease in length, and above the last secondary branch are small, spirally-arranged, and borne on a short narrow terminal axis. As many as five secondary axes emerge from between sheathing leaf bases of enlarged cataphylls, one per cataphyll, with each bearing one or more tertiary branches. Secondary branches stiff, easily broken, possibly six-sided with small scale bracts, ending in a large flower-like cluster of reproductive units.

Tertiary branches short, dividing two or three times, each division immediately bearing a long abaxially recurved conduplicate bract, with a single pedicellate cupule-like megasporophyll in its axil. Two dissimilar leaf-like structures join or fuse with base of megasporophyll: Two inner entire bracts covered with long hairs like the megasporophyll, and two outer digitate and glabrous bracts that are divided near their base into five or six long finger-like projections, each with a stiff central vein.

Secondary branches are terminated by numerous (about eighteen) crowded megasporophylls. The megasporophylls are themselves surrounded by a perianth-like structure. This "perianth" consists of perhaps eight or nine parts resembling the bracts of individual megasporophylls borne on tertiary branches, but the hairy bracts and digitate bracts alternate with one another in

pseudowhorls. Hairy bracts form the outermost "whorl" of the "perianth", and are themselves surrounded by 3-4 long adaxially recurved conduplicate bracts.

Megasporophylls with tapering base, expanding upwards to a rounded apex, and terminated by a bilobed u-shaped collar encircling a small canal or opening into a hollow (frequently sediment filled) chamber. Megasporophylls carpel-like with apical opening extended on open side of u-shaped stigma-like collar to form a suture. Suture short, only extending slightly down the ventral side of megasporophyll. Two shoulder-like bulges flank the apex of immature megasporophylls, but these are much less prominent in larger megasporophylls. Megasporophylls covered with long multicellular and glandular hairs. Epidermal hairs on bulges possibly more pronounced than hairs on surrounding parts of megasporophyll.

Megasporophylls of varying size. The smallest on tertiary branches possessing fully-formed bracts. Largest megasporophylls at least nine times larger than smallest ones. Initially, the bracts and megasporophylls enlarge together, but the bracts around mature solitary megasporophylls are usually damaged and incomplete. Perianth-like structure around each terminal cluster of megasporophylls apparently persistent.

The ovules or seeds and megasporophylls show significantly different stages of development within a single cluster and on tertiary branches. A pair of small anatropous ovules occurs inside much larger ovary-like chamber of megasporophylls of intermediate size; a pair of developing seeds occurs in megasporophylls of nearly full size; a pair of seeds with well-formed seed coats (resistant to compaction) occurs in megasporophylls of mature size. Ontogenetically, megasporophylls rapidly elongated followed by a slower increase in breadth, while ovules or seeds apparently show exponential growth late in megasporophyll development.

DERIVATION: After Daniel I. Axelrod, Professor Emeritus, University of California, Davis, for his pioneering theories on pre-Cretaceous angiosperm evolution, and insight into the diversification and pre-continental drift migration of angiosperms in the Cretaceous.

Axelrodia burgeri Cornet **sp. nov.**

HOLOTYPE: PP34316-PP34319 (one specimen in four parts).
HYPOTYPE: PP34320-PP34321.

DIAGNOSIS: As for the genus.

NUMBER OF SPECIMENS EXAMINED: 3.

ILLUSTRATIONS: Pl. 5, fig. f; Pl. 6, figs. a-c, g-l; Pl. 7, figs. c-e, j-k; Pl. 8, figs. b-c.

DERIVATION: After William C. Burger, Field Museum of Natural History, Chicago, for his progressive revision of the monocot theory of angiosperm evolution, concept of floral evolution from the condensation of simple reproductive units, and

rarely possess them. The occurrence of mainly short segments of secondary branches suggests that they were relatively rigid in life, and were broken and fragmented during burial or compaction of the sediments. The secondary axes appear to have emerged from between the sheathing bases of successive cataphylls, and their spacing in the sediment around the main axis suggests one branch per cataphyll. These axes can be distinguished from associated fern rachises by their parallel folds or grooves, and by the absence of attached fern pinnules.

The main axis of Axelrodia burgeri sp. nov. ends with a relatively short segment of axis (at least 3 cm in length, but incomplete in Pl. 6, fig. a) bearing small spirally arranged scale bracts. This portion of the main axis is slightly wider than the secondary axes, there are no visible grooves, and the scale bracts are more closely spaced than on secondary branches. The reproductive axis appears to have terminated through unequal vascular division, decreasing in width with each emerging secondary branch, but retaining the potential for further growth (i.e. indeterminate growth).

A small but presumably variable number of tertiary branches arise from secondary branches; because of the fragmentary preservation of the secondaries, only proximally or distally-borne tertiary branches can be documented (Pl. 6, fig. k, ax3 adjacent to ax2; see also figure 7c for an interpretation). Terminal reproductive organs typically occur within 5-8 mm of the secondary branches (Pl. 6, fig. a), indicating that tertiary branches are short, and explaining why they are difficult to recognize. Two to three megasporophylls and associated bracts are usually found together in a cluster, suggesting that the tertiary branches divide ultimately almost immediately after diverging from the secondary branches (cf. Pl. 6, figs. g and k). Each megasporophyll-bract unit is subtended by a long (21-24 mm minimum length), abaxially-curved conduplicate bract (Pl. 6, figs. g-h, b2).

Megasporophylls and Associated Structures on Tertiary Branches

The reproductive organs borne on tertiary branches are solitary carpel-like megasporophylls, each of which has its own complement of bracts. Because all the megasporophylls are alike, whether they are borne independently on tertiary branches or in clusters at the ends of secondary branches, they will be described separately below. The enclosing bracts are also similar, but are borne differently for solitary and aggregate megasporophylls. Each solitary megasporophyll is enclosed by at least two tepal-like bracts, which join and fuse with the base of the megasporophyll. Preserved stages of their development indicate that they did not enlarge as rapidly as the maturing megasporophyll (compare figures 5a and 5e), reaching a maximum length of 12-15 mm. These bracts may also have been basally joined or connate, as is hinted at in the only example where two inner bracts (pl) are clearly shown (Pl. 6, fig. h; figure 5e) after the removal of the lower half of the megasporophyll (ms). In most cases, the solitary megasporophyll covers or hides one of these bracts.

The inner bracts are covered with long multicellular(?) hairs, similar to those that cover the megasporophylls (Pl. 7,

fig. c). The hairs are easily visible at a magnification of 4X, but cellular details are unclear. The hairs tend to be oriented in the direction of the bract (figure 5), and frequently diverge outward into the enclosing sediment. The cuticles of the inner bracts, like those of the megasporophylls, are thin and poorly preserved, leaving the thick-walled hairs attached to an organic film that is frequently non-recoverable and destroyed upon acid maceration. There is no evidence of fibers preserved beneath the cuticles.

The inner bracts are partially covered or overlapped by a pair of outer bracts, which appear to join the base of a solitary megasporophyll on opposite sides (Pl. 6, fig. h; figure 5e). The inner and outer bracts form whorls, and it appears that the outer bracts alternate with the inner ones, although this is not particularly clear in the specimens. The outer bracts are much larger than the inner bracts, and divide upwards near their base into five or six long, 1.5-2.0 mm-wide strap-shaped bands, each of which possesses a stiff central vein (Pl. 6, fig. h). In most cases, the outer bracts (p2) can be seen as subparallel to curved bands radiating away from megasporophyll subunits to one side of the inflorescence axis (Pl. 6, fig. a; Pl. 8, figs. b-c); the digitate morphology and disposition of the outer bracts is preserved around an immature or aborted megasporophyll in that specimen (ms* in Pl. 6, fig. a; Pl. 8, fig. c). The free distal bands may reach a length of 20 mm or more, and appear to arise about 4-5 mm above the united base of the bract (these dimensions relate only to mature or nearly mature bracts; figures 5a, 5e, and 5g). During the development of the megasporophyll, the outer

****

Figure 5. a-h. Camera lucida line drawings of Sanmiguelia lewisii megasporophylls and restoration of dispersed seed; all drawings to same scale. -a. Axelrodia burgeri, nearly mature, solitary megasporophyll unit containing two developing seeds (Pl. 6, fig. g). -b. Nemececkigone fabaforma, dispersed seed (Pl. 6, figs. e-f). -c. A. burgeri, immature isolated megasporophyll containing two ovules (Pl. 6, fig. c). -d. A. burgeri, megasporophyll from a cluster terminating secondary branch of inflorescence (Pl. 6, fig. i). -e. A. burgeri, solitary megasporophyll borne on tertiary branch, showing three types of associated bracts (Pl. 6, fig. h). -f. A. burgeri, stamen-like organ found adjacent to specimen in figure 5e (Pl. 6, fig. h, an). -g. A. burgeri, flower-like reproductive unit terminating secondary branch, showing ten megasporophylls, mostly sediment-filled, some with visible ovules or developing seeds inside (Pl. 6, fig. k; also Pl. 7, figs. d-e). -h. A. burgeri, apex to one of the megasporophyll in a secondary branch cluster (Pl. 7, figs. e and j), showing possible veins in stigma-like apex and internal impression of suture along one side. Orientation and preserved density of hairs given on all specimens. Outer digitate tepals given dot pattern. Carbonaceous inclusions or structures shown in black. AX2, secondary axis; B2, subtending conduplicate bract; HI, hilum; MI, micropylar pit; MS, immature megasporophyll; OV, ovule or developing seed; P1, inner hairy tepal of perianth; P2, outer glabrous tepal of perianth; SD, immature seed; SP, shoulder pocket on lateral side of megasporophyll; ST, bilobed stigma-like apex to megasporophyll.

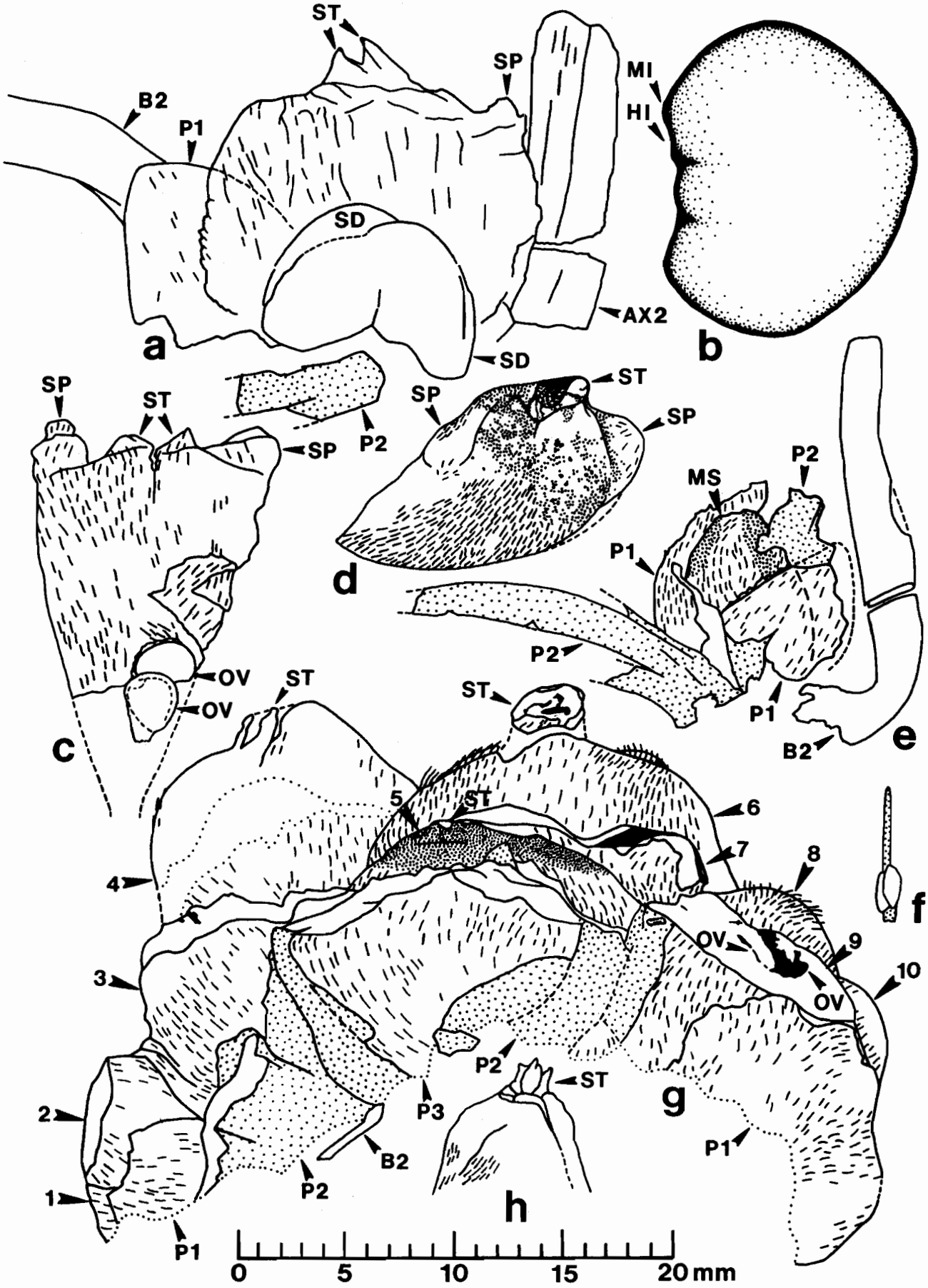
ST
SP
B2
P1
SD
AX2
a
MI
HI
b
SP
ST
P2
SP
c
ST
SP
SP
d
P2
MS
P1
P2
P1
B2
e
OV
OV
ST
ST
5
ST
6
7
8
4
f
OV
9
3
OV
10
P2
ST
P3
g
2
B2
P1
P2
1
h
P1
0
5
10
15
20 mm

bracts may have wilted and fallen off, since they seem to be absent around nearly mature solitary megasporophylls, and sometimes can be found bent downwards away from those megasporophylls (e.g. figures 5a and also 7c for a reconstruction).

The outer bracts can be distinguished from the inner ones even as incomplete segments because of their glabrous cuticle, which shows no signs of epidermal hairs. Even though the cuticle is thicker, it does not preserve much better than that of the inner bracts, and it was evidently only thinly cutinized. Consequently, acid maceration produces very few identifiable fragments of cuticle from these bracts. The contrasting difference between inner and outer bract cuticles made it possible to trace or follow these structures under magnification, even where they overlapped (cf. figure 5).

In addition to the perianth, one isolated stamen-like organ with a laminar base and long filamentous apex was found intimately associated with portions of two megasporophylls and their bracts (Pl. 6, fig. h, an; figure 5f). Dissection of the two elliptical bodies joined to the filament produced only ovoid cells similar in size to the pollen of Synangispadixis tidwellii **sp. nov.** The distal filament to the stamen-like organ (not visible in the photograph) is oriented subparallel to the digitate bands of the outer bracts, and is directed away from the basal portion to a second megasporophyll (Pl. 6, fig. h); this association-orientation raises the possibility, at least, that the megasporophylls and their associated bracts were either bisexual, or possessed staminodia - an indication of an ancestral bisexual condition. Since no other stamen-like organs were found, the identity and attachment of this organ to the outer bracts must remain conjectural at this time. More information concerning the possible manner of attachment of such an organ will be addressed in the description below of clusters of megasporophylls and their perianth-like parts terminating secondary branches.

Clusters of Megasporophylls on Secondary Branches

The flower-like reproductive units borne terminally on secondary branches of the inflorescence consist of clusters of carpel-like megasporophylls surrounded by a perianth-like structure composed of bracts (Pl. 6, figs. k-l; Pl. 7, figs. d-e; figure 5g and also figure 7c for a reconstruction). The number of megasporophylls, and consequently the size of the clusters, may vary; along the distal portion of the inflorescence axis (Pl. 6, fig. a) these units appear as compressed and distorted masses of overlapping megasporophylls and bracts. Some of the flower-like units appear to have no more than ten megasporophylls; however, it is difficult to impossible to distinguish the outlines and identities of all parts, since most of the megasporophylls collapsed - either because they were damaged or before they could be filled with sediment. Some of them broke apart during burial and compaction, yielding isolated megasporophylls (Pl. 6, fig. c; Pl. 8, fig. b, large arrows). An informative specimen of a flower-like unit, however, was fossilized after the megasporophylls became filled with clay and silt, which preserved the integrity and shape of some carpel-like parts.

The apical flower-like unit had from ten to eighteen carpel-like megasporophylls at its center, but may have had more. An isolated specimen preserved in three dimensions (Pl. 6, figs. k-l) will serve as the example: Unlike the solitary megasporophylls borne on tertiary branches, the megasporophylls of the flower-like unit appear to lack individual bracts. Instead, they are collectively surrounded by an estimated eight or nine inner bracts, some of which are hairy and others of which are glabrous. There is also the possibility that some of the outermost megasporophylls alternated with the bracts, since an ordered phyllotaxy of individual whorls is not evident. The inner series of bracts in turn is surrounded by three or four conduplicate bracts (see figure 7c for an interpretation). Sediment fills the gaps between the perianth-like parts, and allows them to be individually followed (Pl. 7, fig. d). Most of the hollow megasporophylls were filled with sediment, and some were transversely broken. Cross sections of megasporophylls can be distinguished from the hairy bracts by the manner in which their walls completely surround a central chamber, and by the remains of ovules or seeds preserved within those chambers (Pl. 6, fig. k; Pl. 7, fig. e; figure 5g).

All of the floral parts appear to be attached to a receptacle, or swollen secondary branch apex (Pl. 6, fig. 1). The hairy simple bracts and glabrous digitate bracts apparently alternated with one another, forming a close spiral resembling a perianth around a cluster of megasporophylls (figure 5g). This change in arrangement brings some of the digitate bracts into contact with the megasporophylls, a condition not observed for megasporophylls on tertiary branches. In addition, some hairy simple bracts overlap and lie outside the glabrous digitate bracts. The exact number of bracts cannot be determined from the available specimens, but three hairy bracts and two glabrous bracts can be clearly distinguished on one side of the flower-like unit (figure 5g and also figure 7c for a reconstruction).

The digitate part or strap-like bands of the glabrous bracts are not preserved in the portion of the specimen recovered (Pl. 6, fig. k; Pl. 7, figs. d-e). The bases of those bands, however, are preserved and appear as vertical folds and overlapping flaps of cuticle (figure 5g). The glabrous bracts possess an additional flap of tissue on their basal adaxial side, which is not identifiable as one of the strap-like bands (figure 5g, p2). This flap was not identified on the bracts associated with solitary megasporophylls, probably because of insufficient material. The isolated stamen-like organ (staminodium?) found associated with a pair of solitary megasporophylls (Pl. 6, fig. h; figures 5e-5f) may have been attached to such a flap. Until more specimens are found and the identity of this flap is established, its function and significance remain obscure. Therefore, the reconstruction in figure 6c shows the flap only as it is preserved in the specimen.

The Megasporophyll

The megasporophylls have a narrow base that expands upwards to a broad rounded apex possessing a terminal stigma-like process (Pl. 6, figs. a and i; figures 5c and 5d). The megasporophylls

cotyledon-like organs, a plumule or epicotyl between the bases of the cotyledons, an elongate hypocotyl, and a radicle or root cap next to the hilum where the micropyle would have been (figure 7b). The cotyledons are of distinctly different sizes, with the larger one filling the convex side of the seed, and the smaller one tucked in the curl of the larger cotyledon. The large amount of carbonaceous residue and the size of the casts suggest that the cotyledons were fleshy.

DISCUSSION: The presence of similar seeds at both the type locality in Colorado and at Sunday Canyon in Texas supports the interpretation that the fossils described in this paper belong to one plant, Sanmiguelia lewisii Brown. Only with additional data will it be known whether these seeds are peculiar only to Axelrodia and Sanmiguelia. A bean-shaped seed with one side flatter than the other, and a micropylar pit adjacent to the hilum might suggest the presence of a u-shaped dicotyledonous embryo with one cotyledon smaller than the other. The embryo cast demonstrates that the superficial characteristics of the seed reflect the general morphology of the embryo.

THE HABITAT AND HISTORY OF ONE SANMIGUELIA COLONY

The sedimentary sequence in which Sanmiguelia is preserved indicates changing habitat conditions. The sequence begins with a paleosol, in which the vertical stems are firmly anchored by roots; primary and secondary roots can be traced downwards at least 8 cm (figure 2). Three clusters of two to four vertical axes were uncovered during excavation. They were spaced 175 cm and 85 cm apart. Two clusters are illustrated in figures 2a and 2b. The paleosol gradually rises in elevation to the west, where it is truncated by a channel fill sequence (figure 1). Several ferns were preserved adjacent to the westernmost cluster of axes. Their fronds were found on top of the paleosol, and fern rhizomes and roots could be followed in the paleosol. Only one type of fern leaf was found, which is assignable to Cladophlebis cf. C. macrophylla Fontaine. Associated with the sterile fronds were fertile spikes containing thousands of spores assignable to Cyclotriletes margaritatus Mädler (1964).

Above the paleosol a 1-5 cm thick layer of dark gray shale could be followed for a short distance down slope, where the shale is replaced by mudstone. C. margaritatus is the most common dispersed spore in the shale, even though a diversity of other spore types is also present. The shale thickens and thins as the overlying layer of pinkish-buff siltstone (layer S1 in figure 2) intrudes down into it. In some places siltstone load-casts distort and deform the underlying shale layer, and also the fossil plants the shale contains. Within the shale well-preserved plicate leaves assignable to Sanmiguelia were found. Many of these leaves were large, although they were frequently folded and ripped either during burial or during rapid loading of the soft mud matrix by the overlying siltstone, resulting in uneven compaction and diaperic movement (Pl. 1, fig. c). Post-depositional movement is evidenced by very small slip surfaces or faults displacing portions of the same leaf.

The pinkish-buff siltstone layer (S1 in figure 2) above the shale varies from 3 cm to 5 cm in thickness. Some of the vertical axes ended abruptly at the top of layer S1, while others continued through it. Layer S1 is overlain by a 14-18 cm thick gray shaley siltstone layer (S2), which becomes a dark gray shale to the west (up depositional dip), and a gray mudstone to the east. Three vertical stems ended abruptly at the top of layer S2, while at least two stems were followed upwards to the overlying conglomeritic sandstone. Two pinkish-buff to grayish-buff sandy siltstone layers (S3 and S4) overlie layer S2. A depositional surface separating these two layers was recognized by bends in the vertical axes that pass through them. One of the axes appears to have terminated at this surface, with a side branch continuing the upwards growth of the plant (Pl. 2, fig. b).

A cluster of Sanmiguelia leaves was found terminating a vertical axis at the top of the siltstone sequence by Paul E. Olsen (1981, personal communication), and deposited in the Yale Peabody Museum collection. The apical leaves were reported by Olsen to be smaller than the leaves lower on that axis, as Tidwell et al. (1977) noted for their Colorado specimens. From about the same stratigraphic position another leaf was found overlapping a specimen of Synangispadixis tidwellii **sp. nov.** (Pl. 4, fig. a). Both of these specimens suggest that the stems did not extend much higher. Tidwell et al. (1977) report axes measuring at least 61 cm in height. The maximum length of stems preserved at the Sunday Canyon locality is 65 cm.

The environment in which Sanmiguelia grew appears to have bordered a meandering river channel (Olsen, 1985). Initially, a colony of Sanmiguelia grew side by side with ferns in soft water-soaked soil at the edge of an interdistributary lake or pond. Soon after the colony established itself through an extensive rhizome system, the margin of the lake began to encroach upon the colony, and an organic-rich mud layer was deposited on top of the paleosol. The ferns were apparently killed off by the rising water, but Sanmiguelia continued to grow. Some wind(?) torn leaves fell off the stems into the mud, where they were preserved along with the ferns.

The first pinkish-buff siltstone layer (S1) was probably deposited as a turbidity current distal to a crevasse splay during a flood (Olsen, 1985). Some large stems bearing an Axelrodia burgeri **sp. nov.** inflorescence were knocked down by this high energy event, and were found sandwiched between the siltstone and the underlying dark gray shale. Either rising water or flood damage ended the growth of some of the vertical axes, while others continued to grow and repair themselves. Those axes that died were broken off before or during the next flood, while new shoots propagated upwards from the bases of damaged stems or from rhizomes. Each successive flood added a new layer of sediment (S1-S4, figure 2), and with each deposit some stems were irreparably damaged. Many of Sanmiguelia's leaves were ripped and torn off during the floods, and their fragments can be found randomly distributed throughout the siltstone layers. With the loss of leaves, continued growth and survival depended on the preservation of apical and lateral shoot meristems, which were probably protected by sheathing leaf bases. Its sturdy stems, regenerative capacity, and growth along the

margins of a lake indicate that Sanmiguelia was probably well adapted for climatic extremes in a fluvial red bed environment frequented by floods.

COMPARISONS WITH FOSSIL PLANTS

There are several fossil plants described in the literature that are similar to Sanmiguelia and its probable reproductive structures: The secondary axes of Synangispadixis tidwellii **sp. nov.** with their aggregation of sporangia (microsporophylls) compare with the microsporangiophores of the latest Triassic Irania hermaphroditica (Schweitzer, 1977), which are borne below megasporophylls on the same axis. Unlike Synangispadixis, however, the microsporangia are stalked and the stalks terminate with two suspended ellipsoidal pollen sacs. The megasporophylls are spirally arranged and consist of a pair of capsules at the ends of a dichotomized branch. Each capsule consists of a pair of basally joined megasporophylls bearing about six ovules each on their adaxial or facing sides. The morphology of the megasporangiophores differs considerably from the megasporophylls and associated structures of Axelrodia burgeri **sp. nov.** The synangia-like morphology of the microsporangiophores and the paired decussate morphology of the megasporangiophores in Irania compare more with similar structures in the Gnetales (e.g. Ephedra) than with Synangispadixis, Axelrodia, or the angiosperms. In addition, Desmiophyllum armanii, the leaves associated with Irania, have parallel veins that end blindly at the distal margin, and show no tendency toward apical vein fusion as in Sanmiguelia.

Terminal seed-bearing axes that superficially resemble large gymnospermous cones have been described from the Richmond Basin coal measures of Virginia. The Richmond Basin sequence has been more recently dated as early to middle Carnian in age (Cornet and Olsen, 1985). Fontaine (1883) originally described these axes under the name, Zamiostrobus virginiensis, and considered them to be cycad cones (Fontaine, 1883, p. 85, Pl. XLVII, figs. 4, 5). Bock (1954) renamed them, Primaraucaria wielandii, and compared them to the cones of araucarian conifers. Later, Bock (1969) reported finding about 200 specimens, and indicated that they were a common element in the Winterpock coal flora, where they were associated with Podozamites tenuistriatus Fontaine, large Macrotaeniopteris and Eoginkgoites leaves, large fern fronds, and giant Equisetites stems.

Four specimens of these fruits were obtained from the Philadelphia Academy of Natural Sciences, where Bock had deposited them. The most striking evidence against a coniferalean affinity is their non-woody stems and reproductive axes that lack a carbonaceous core (Pl. 9, figs. b, d, and h). Large ovoid compound fruits are borne at the ends of long unbranched pachycaul stems, which are completely covered with large, closely-spaced,

****

Figure 9. **a-c.** Zamiostrobus virginiensis **Fontaine** 1883 or Primaraucaria wielandii **Bock** 1954 sensu lato. Reconstructions of three different types of fruiting heads and reproductive structures illustrated by Bock (1969) under P. wielandii. **-a.** TYPE A. **-b.** TYPE B. **-c.** TYPE C. See text for further descriptions; scale in cm: x 2.

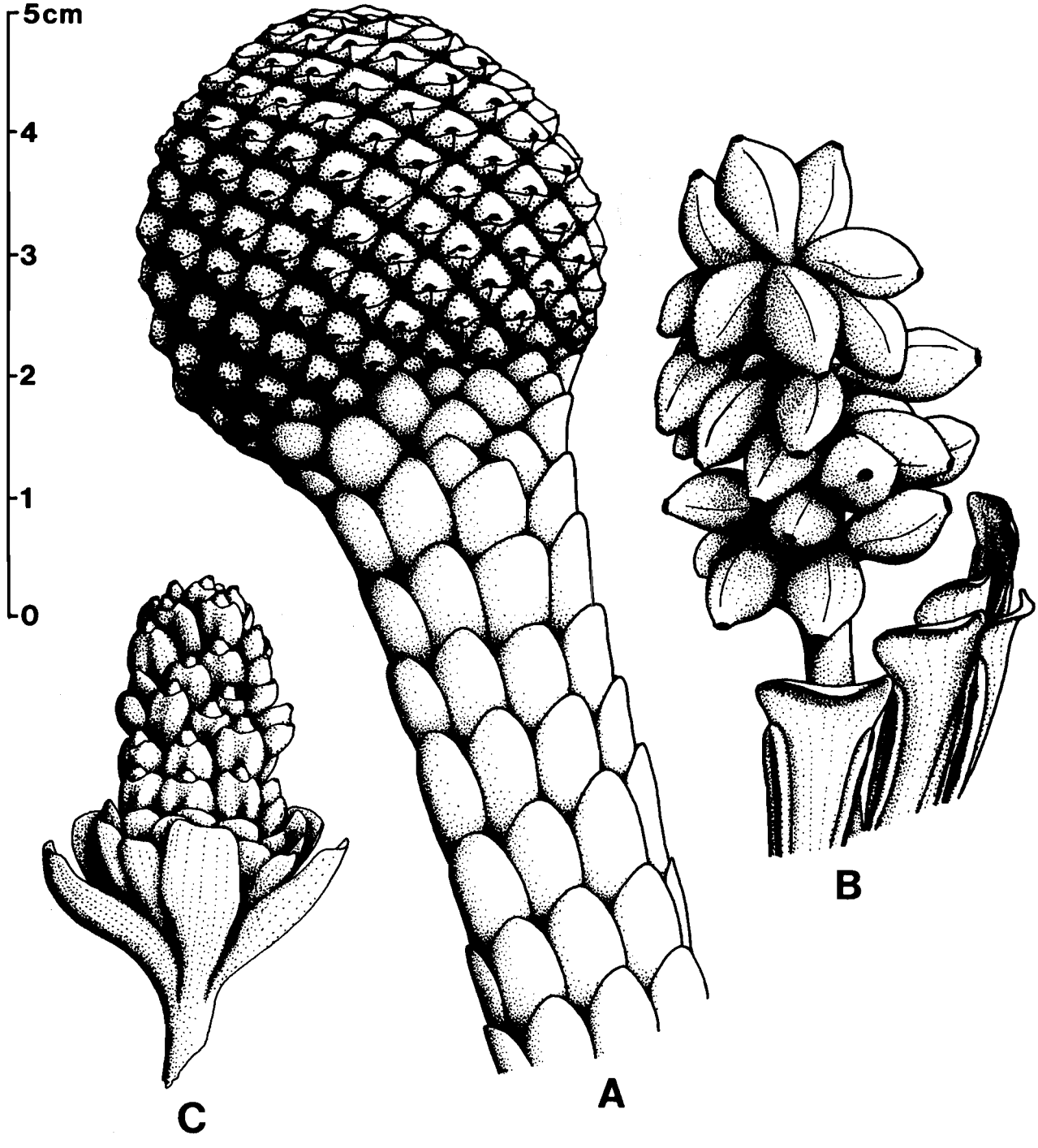
5cm
4
3
2
1
0
A
B
C

spirally-arranged and overlapping leaf-like bracts (Pl. 9, fig. b; Bock, 1969, figs. 528-530, 535; Bock, 1962, figs. 470-471). At least three different types of reproductive structures are here recognized: Bock's species includes several similar and apparently closely related reproductive axes (figures 9a-9c). Fontaine's specific epithet takes priority for at least one of these reproductive axes, while Bock's generic name may have to be retained if his holotype cannot be linked to a Fontaine species.

One of these cone-like structures (**Type A**) superficially resembles a pineapple in that each spirally-arranged megasporophyll is subtended by a long conduplicate bract that visibly overlaps the apex of the megasporophyll (Pl. 9, fig. a, b2; figure 9a). Another reproductive axis (**Type B**) resembles a giant magnolian fruit with subtending latrorse laminar stamens (PL. 9, fig. h, 11s; figure 9b), while a third (**Type C**) possesses a wide undifferentiated collar of expanded bracts at the base of a long axis bearing megasporophylls in the axils of large bilobed bracts (figure 9c; Bock, 1969, fig. 536; Bock, 1962, fig. 470b). All of these reproductive axes resemble the flower-like units terminating secondary axes of Axelrodia burgeri **sp. nov.**, but most have many more carpel-like parts. The perianth-like parts or bracts subtending the solitary megasporophylls of Axelrodia are present in some but not all of the "Primaraucaria" or "Zamiostrobus" fruiting structures. Even though the megasporophyll subunits are united to a common axis, they are individually attached by means of elongate pedicels or secondary branches. They are not borne on tertiary branches as in A. burgeri (Pl. 9, figs. b, d, and h). The long bract-clad axis supporting these fruiting heads may be similar to the slender secondary axes of Axelrodia burgeri **sp. nov.**, but the analogy is uncertain, and a comparison with the long stout primary axes of Axelrodia is equally plausible.

The megasporophylls of reproductive axis **Type B** are about 14-16 mm long, solitary, without subtending bracts, spirally arranged, and pedicellate (Pl. 9, fig. h; figure 9b). Their distally expanding shape, rounded apex, conical stigma-like pore (Pl. 9, fig. i, st), and paired ovules or seeds (Bock, 1969, fig. 545) compare closely with the carpel-like megasporophylls of Axelrodia. The ovules or seeds are enclosed within a cuticularized ovary wall, the only access to which was through the pore at the conical apex, which may represent the base of a longer deciduous structure. The apparent construction of the megasporophyll differs significantly from that of the reflexed "cupule" of Caytonia, which has a small lip or opening on one side close to the stalk and ovules that reached maturity with functional micropyles. In addition, the megasporophylls of "Primaraucaria" Type B were apparently shed at maturity, since they were found by Bock as isolated elements in the sediment (Bock, 1969, fig. 545). Unlike Axelrodia, the megasporophyll cuticle is glabrous proximally and papillate distally (Pl. 9, fig. i; figure 10h). The basally-narrowing laminar stamen-like microsporophylls that subtend the reproductive axis are 5-8 mm wide and exceeded 17 mm in length. Each bears two very long anther-like sacs, one on each side. These sacs are covered with a specialized cuticle that is continuous with that of the lamina, and remnants of a possible tapetum were found inside; no pollen was found, since the microsporophylls had dehisced, and only one chamber was present at maturity (as

in many angiosperm anthers).

The megasporophylls of reproductive axis **Type A** are diamond-shaped in cross section, and arranged in a tight spiral (Pl. 9, figs. a and b; figure 9a) around a non-woody primary axis at the center of numerous decurrent secondary axes (Pl. 9, fig. d). The mass of megasporophylls is ellipsoidal and borne at the apex of a main axis bearing large bracts (Bock, 1969, figs. 534, 539). There is an abrupt transition from megasporophylls to large bracts, with no specialized perianth or pollen-bearing organs. The bracts possess a papillate cuticle with anomocytic stomata. The megasporophylls are wider basally than those of reproductive axis **Type B**, and contain more seeds. The fruiting head collapsed during fossilization to form a 2 mm thick compression, mainly composed of multiple layers of cuticle and enclosed seeds. The only opening to the megasporophyll is a conical apical pore, visible on surface impressions of the cone-like fruit (Pl. 9, fig. a, st). The apex superficially resembles a cone scale umbo.

A portion of the coalified compression to one specimen (Pl. 9, fig. b, at *) was removed, oxidized, cleared in NaOH, embedded in paraffin, and sectioned. The mounted thin sections showed thick-walled seeds completely surrounded by a pair of cuticles, which were separated by as many as two additional pairs of cuticles belonging to surrounding bracts (cf. Pl. 9, fig. d, b2?). Some of the accessory cuticles fuse with the base of the megasporophyll, but are free apically, indicating that they may represent perianth-like parts similar to those around the solitary megasporophylls of Axelrodia. The cuticle of the subtending "conduplicate" bract typically has large epidermal cells with thick cell walls, and can be distinguished from the cuticles of the megasporophyll and adnate accessory cuticles (compare Pl. 9, fig. c with Pl. 9, figs. d-e). One immature and possibly aborted megasporophyll subunit showed an outer bract completely surrounding the collapsed and highly folded cuticles of a megasporophyll, which contained at least four elliptical cuticles of possible ovules in cross section.

The enclosed oval seeds possess a thick granular wall in cross section that strongly stains with safranin O. Isolated seeds, measuring 2.6-2.8 mm in length by 1.6-2.0 mm in width, were removed from dissected megasporophylls; they showed no signs of a micropyle, showing only two shallow pits at one end (Pl. 9, fig. g, arrows). Their walls are typically strongly wrinkled, and there was no pollen found inside the ovary or attached to the seeds. However, small monosulcate pollen was found clinging to the outer distal surface of the megasporophyll. One immature or aborted seed was found with micropyle preserved, and a hilum that lay adjacent to the micropyle (Pl. 9, fig. f, mi and hi); no pollen was present in the micropyle. No funiculus was preserved and the mature seeds appear to lie loosely within the ovary. Upon dissection of the cuticles, one aborted anatropous ovule, 250 um wide, was discovered still attached by means of a short stalk to the inner cuticle of the megasporophyll (Pl. 9, fig. e).

The absence of pollen within the ovary, and ovules that lost their micropyles during development suggest that pollen germination took place outside the ovary and that ovules did not develop to maturity until fertilized. The similarity of the carpel-like megasporophylls and their subtending leaf-like parts to those of

Coincidentally, secretory hydathodes may have evolved at the leaf apex (Melville, 1962), exudates of which facilitated pollen capture and transportation in fluid drops. As the drops ran down the axis of the leaf to the ovules, they supplemented the function of pollen drops at the ends of one or more micropylar tubes; selection increased the amounts of nutrient in the fluid, allowing pollen tubes to grow increasing distances to the ovules. Eventually, a specialized mucilage-coated transmission tissue evolved from the leaf apex down into the ovary, and the ovules evolved strong pollen-tube attractants that produced a chemical gradient in the fluids and mucilage coating the ovary wall.

The genetic suppression of the ovule-bearing axis may have extended to the ovules, thereby setting the stage for post-fertilization growth and endosperm development. As the ovule-bearing axis became suppressed, ovules attached to the ventral or adaxial side of the sheathing leaf base, because that is the side closest to the axis, and because a wide central vein ran down the decurrent dorsal or abaxial side. The leaf apex became reduced in size as transmission tissue became more effective (figure 10e), but it retained the venation of a leaf in a condensed form because of the specialized needs of the glandular stigma (figure 7a; cf. Melville, 1962). The bilobed morphology of the stigma (an angiosperm characteristic) may have resulted from the premature loss of the apical meristem, a typical characteristic of Sanmiguelia leaves. The anthers developed in a similar manner as the carpels, but because the leaf blade was superfluous and non-functional, it was completely lost (figure 10c).

The conduplicate carpel has long been considered the primitive form within the Ranales, and the basis for carpel evolution in the angiosperms (Bailey and Swamy, 1951). The concept arose out of the similarity of the carpel of Drimys piperita (Winteraceae) to a folded leaf with three veins. The primary distinction between the conduplicate theory of carpel evolution and the sheathing leaf base theory presented above is whether a leaf blade joined with and wrapped around an ultimate ovuliferous branch, or whether the ovuliferous branch contracted into the basal tube of a sheathing leaf. However, the conduplicate theory assumes that a pollen-tube transmission tissue evolved after micropylar extensions were lost and after the sides of the leaf came together, and that ovules were initially attached near the margins of the leaf (as in some Paleozoic pteridosperms and cycads; Doyle and Donoghue, in press). Relatively few examples are known outside the angiosperms where pollen germinates on non-integumentary organs; in Araucaria (Doyle, 1945), and perhaps also in some Mesozoic Cheirolepidaceae, which have megasporophylls of similar construction, the pollen germinates on the ovuliferous scale. Once the conduplicate leaf was closed, there would be no dual mechanism of bringing the pollen near the egg as with the sheathing leaf base theory, which allows for the gradual evolution of a pollen-tube transmission tissue and the loss of a micropylar tube. The megasporophyll of Glossopteris folded and enclosed small ovules in accordance with the conduplicate theory, but specialized micropyles communicated with the opening along the suture, and the ovary became filled with a cancellous tissue (Gould and Delevoryas, 1977).

Angiospermous fruiting heads from the Richmond Basin of Virginia (see figure 9, and comparison with fossil plants above) possess pedicellate carpels similar to those of Axelrodia and Archaeanthus Dilcher and Crane (1984), but the stigmatic regions of those cone-like fruits are restricted to the apical or distal ends of the carpels, and form no part of the ventral or adaxial surface. Ventral paired stigmatic crest may not have evolved until after enclosing perianth parts were lost and the number of paired ovules greatly increased along the ventral side of the carpel (figures 10f-10i). The condensation of many megasporophyll subunits into a strobilus-like flower, a sequential loss of perianth parts around each floral subunit (figures 10f-10i), and the evolution of laminar stamens which subtend the carpels on the same axis (Pl. 9, fig. h) may have lead to an early evolutionary specialization within the angiosperms, whose descendants are grouped today in the Magnoliales. Perhaps that is why the Drimys-type conduplicate carpel is unknown for the monocots, and why the apocarpous carpel with an apical stigma is found in Sanmiguelia. Burger (1980) anticipated the discoveries presented here in his analysis of angiosperm floral evolution:

"Unfortunately, a strobilus-like flower in an ancient and relictual order is no guarantee that this kind of flower is the single ancestral type from which all other contemporary flowers descended. The flowers of the Magnoliaceae may represent some early experiments in floral organization; they need not have been the archetype from which all other flowers have evolved. The diversity of floral organization within the Magnoliales and the closely related Laurales suggests that they include a variety of basic floral plans, ranging from the long floral receptacle of the Magnoliaceae and the cupulate receptacles so common in the Laurales to the very simple flowers of the Chloranthaceae. This diversity of floral architecture within the Magnoliales and related orders supports the idea that contemporary flowers may be polyphyletic; that is, made up of homologous parts that have come together to form flowers in different ways in different lineages. There is a variety of evidence supporting this point of view. Both floral ontogeny, floral structure, and chemistry are very distinctive in the Magnoliales, implying that they are an early side branch of angiosperm evolution rather than a basic stem group" (Burger, 1980, p. 1).

REASONS FOR A POOR PRE-CRETACEOUS ANGIOSPERM RECORD

Axelrod (1952) originally proposed a theory that angiosperm history extended back to the Permo-Triassic, perhaps to pre-magnolian proangiosperms, and that an upland origin could explain their poor pre-Cretaceous fossil record. Scott, Barghoorn, and Leopold (1960) countered by stating that all records of pre-Cretaceous angiosperms are suspect, and that angiosperms arose in the Middle Mesozoic. Axelrod (1961) rebutted their ideas, and later extended his theory (Axelrod, 1970) to include the effects of ocean-floor spreading on early angiosperm history, interpreting the transtropical distribution of many angiosperm families as indicating a pre-Cretaceous origin. Doyle (1977; 1978) and Hickey (Hickey and Doyle, 1977) followed Scott, Barghoorn, and Leopold's lead with a detailed study of patterns of evolution of

_____, 1975, The Chinle (Upper Triassic) flora of southeastern Utah, Four corners Geol Soc. Guidebook, 8th Field Conf., p. 143-147.

_____, 1976, Occurrence of the controversial plant fossil Sanmiguelia in the Upper Triassic of Texas, Jour. Paleont., V. 50, No. 5, p. 799-804.

_____, 1978, Stratigraphy of the Ciniza Lake Beds and related strata, in Geology, paleontology, and paleoecology of a Late Triassic lake, western New Mexico, S. R. Ash, editor, Brigham Young Univ. Geol. Studies, V. 25, Part 2, p. 1-14.

Axelrod, D.I., 1952, A theory of angiosperm evolution, Evolution, V. 6, No. 1, p. 29-60.

_____, 1961, How old are the angiosperms?, Amer. Jour. Sci., V. 259, p. 447-459.

_____, 1970, Mesozoic paleogeography and early angiosperm history, Bot. Rev., V. 36, No. 3, p. 277-319.

Bailey, I.W. and B.G.L. Swamy, 1951, The conduplicate carpel of dicotyledons and its trends of specialization, Amer. Jour. Bot., V. 38, p. 373-379.

Barghoorn, E.S.Jr., 1940, The ontogenetic development and phylogenetic specialization of rays in the xylem of dicotyledons. I. The primitive ray structure, Amer. J. Bot., V. 27, p. 918-928.

Becker, H.F., 1964, Paleobotanical exploits in Colorado and Kansas, Garden J. (N.Y.B.G.), V. 14, No. 6, p. 231-233.

_____, 1972, Sanmiguelia, an enigma compounded, Palaeont. Abt. B, V. 138, p. 181-185.

Bock, W., 1954, Primaraucaria, a new araucarian genus from the Virginia Triassic, J. Pal., V. 28, p. 32-42.

_____, 1962, Systematics of dichotomy and evolution, Geol. Cntr. Res. Ser., North Wales, PA, V. 2, 300 pp.

_____, 1969, The American Triassic flora and global distribution, Geol. Cntr. Res. Ser., North Wales, PA, Vs. 2-3, 406 pp.

Brown, R.W., 1956, Palm-like plants from the Dolores Formation (Triassic), southwestern Colorado, U.S. Geol. Surv. Prof. Pap. 274-H, p. 205-209.

Burger. W.C., 1977, The Piperales and the monocots. Alternate hypotheses for the origin of monocotyledonous flowers, Bot. Rev., V. 43, No. 3, p. 345-393.

_____, 1980, On the origin of flowers, IAAP Newsletter, V. 6, No. 1, p. 1-2.

_____, 1981, Heresy Revived: The monocot theory of angiosperm origin, Evol. Theory, V. 5, p. 189-225.

Chamberlain, C.J., 1966, Gymnosperms, structure and evolution, Dover Pub., Inc., NY, 484 pp.

Cornet, B., 1977, The palynostratigraphy and age of the Newark Supergroup, unpublished Ph.D. thesis, The Pennsylvania State University, 505 pp.

_____, 1979, Angiosperm-like pollen with tectate-columellate wall structure from the Upper Triassic (and Jurassic) of the Newark Supergroup, U.S.A., Palynology, V. 3, Abstr., p. 281-282.

_____, 1980, Tropical Late Triassic monosulcate and polysulcate angiospermid pollen and their morphological relationship with associated auriculate polyplicate pollen, 5th International Palynological Conference, Cambridge 1980, Abstr., p. 91.

_____, 1981, Recognition of pre-Cretaceous angiosperm pollen and its relationship to fossil polyplicate pollen, Palynology, V. 5, Abstr., p. 212-213.

_____, in press, Triassic and Jurassic pollen with angiospermous affinites, A.A.S.P. Contribution Series, 101 pp.

_____ and P.E. Olsen, 1985, A summary of the biostratigraphy of the Newark Supergroup of eastern North America with comments on Early Mesozoic provinciality, in III Congreso Latinoamericano de Paleontologia. Mexico, R. Weber, editor, Simposio sobre Floras del Triassico Tardio, su Fitogeografia y Paleoecologia. Memoria, p. 67-81.

Crane, P.R., 1985, Phylogenetic analysis of seed plants and the origin of angiosperms, Ann. Missouri Bot. Gard., V. 72, No. 4, p. 716-793.

_____ and D.L. Dilcher, 1984, Lesqueria: an early angiosperm fruiting axis from the mid-Cretaceous, Ann. Missouri Bot. Gard., V. 71, No. 2, p. 384-402.

Dahlgren, R.M.T.; H.T. Clifford, and P.F. Yeo, 1985, The families of the monocotyledons, structure, evolution, and taxonomy, Springer-Verlag, NY, 520 pp.

Dickison, W.C., 1975, The bases of angiosperm phylogeny: vegetative anatomy, Ann. Missouri Bot. Gard., V. 62, p. 590-620.

Dilcher, D.L. and P.R. Crane, 1984, Archaeanthus: an early angiosperm from the Cenomanian of the western interior of North America, Ann. Missouri Bot. Gard., V. 71, No. 2, p. 351-383.

Walker, J.W. and A.G. Walker, 1984, Ultrastructure of Lower Cretaceous angiosperm pollen and the origin and early evolution of flowering plants, Ann. Missouri Bot. Gard., V. 71, No. 2, p. 464-521.

Plate 1, figs. **a-h**. Sanmiguelia lewisii Brown. **-a**. PP34363. Fallen axis with two small leaves attached, showing sheathing leaf base (slb). **-b**. Enlargement of fig. a showing leaf plications, torn leaf apex, and free part to sheathing leaf base (slb). **-c**. PP34359. Folded distal portion of a large vegetative leaf, showing well-preserved parallel venation and elongate resin bodies (arrows). **-d**. SLIDE-118. Acetate transfer of leaf showing elongate resin body over a vein; x 81. **-e**. SLIDE-118. Acetate transfer of leaf showing annular-helical tracheids of a quaternary vein; x 370. **-f**. Lower half: Helical-scalariform tracheids macerated from inner part of secondary xylem; x 300; Upper half: THIN SECTION-122. Helical-scalariform tracheid in a silicified protoxylem bundle of inflorescence axis to S. tidwellii for comparison; x 450. **-g**. Acetate transfer of basal portion of leaf showing bifurcating secondary veins within a dividing primary vein; portions of coalified veins removed during transfer, leaving white areas and underlying cuticle exposed; x 20. **-h**. Acetate transfer of basal portion of leaf showing secondary veins diverging laterally and interconnected by cross veins (arrows); x 20.


a
sfb
0 cm 1 2
b
0 cm 1 2
sfb
c
0 cm 1 2 3 4
d
e
f
g
h

Plate 2, figs. **a-k**. Sanmiguelia lewisii Brown. **-a**. PP34337. Portion of a vertical axis, showing striate pith cast, limonitic petrifaction of secondary xylem with divergent leaf trace exposed, and sheathing leaf base separated from stem by a sedimentary cast of space in axil of leaf. **-b**. PP34338. Portion of a vertical pith cast, showing a secondary branch diverging upwards from below the broken end of main axis, and portion of a leaf sheath separated from carbonized remains of stem by sediment; see figure 2. **-c**. THIN SECTION-S10 of PP34355. Transverse section of a limonitic root petrifaction, showing increasing heterocellular pattern from center of stele (below) to cambium (above), and vessel elements (v) interdispersed between smaller tracheids; x 92. **-d**. THIN SECTION-S12 of PP34355. Tangential section of root, showing crowded simple pits, narrow tracheids, and a string of wider vessel elements (v) with indications of porous end plates (arrow); x 92. **-e**. Enlargement of fig. c, showing scalariform end plates visible within some of the tracheids; note simple pits on side walls; x 230. **-f**. SLIDE-121. A specimen of Succinctisporites cf. S. circumdatus Leschik found clinging to leaf cuticle; 75 um tall by 38 um wide. **-g**. SLIDE-118. Acetate transfer of leaf, showing abundant stomata, most of which are oriented perpendicular to veins; x 81. **-h**. SLIDE-120. Acetate transfer of basal portion of leaf, showing a primary vein flanked by numerous tertiary veins; x 3.7, note scale. **-i**. SLIDE-118. Enlargement of an elongate resin body in leaf (see also Pl. 1, fig. e.); x 370. **-j**. SLIDE-118. Acetate transfer of leaf, showing a short quaternary cross vein, and a parallel quaternary joining a wider quaternary to form a tertiary vein; x 90. **-k**. SLIDE-118. Acetate transfer of leaf showing a rare tertiary cross vein; x 90.


a
0 1 2 cm
b
0 1 2 cm
CAMB
v
c
v
d
e
f
g
h
i
j
k

Plate 3, figs. a-e. Synangispadixis tidwellii Cornet sp. nov.; figs. f-i. Sanmiguelia lewisii Brown. -a, S. tidwellii, HOLOTYPE: PP34322. Nearly complete specimen, showing naked axis (extending basally another 1.6 cm on counterpart) with numerous spirally arranged synangia-like secondary axes, which bear dehisced biloculate microsporophylls on expanded "fleshy" axes proximally (below arrow), and pollen-bearing immature secondary axes distally (above arrow); individual vascular strands containing helical-scalariform tracheids (a': x 400) can be seen at base of axis. -b. S. tidwellii, PP34327. Enlargement showing "fleshy" secondary axes bearing hundreds of sediment-filled (dehisced) microsporophylls; x 3. -c. S. tidwellii, HOLOTYPE: PP34322. SEMG of an immature microsporophyll, showing enlarged endothecial cells preserved along suture margins, thin (damaged) side exposing an enclosed pollen mass, proximal wrinkled cuticle over smaller endothecial cells, and short narrow base; note 100 um scale (see also figure 3f). -d. S. tidwellii, SLIDE-101 of PP34322. A clump of monosulcate pollen grains removed from one of two pollen masses in each biloculate microsporophyll; clump 60 um wide, top grain 26 um long. -e. S. tidwellii, SLIDE-101 of PP34322. Two monosulcate pollen grains; 24 x 18 um and 24 x 16 um. -f. Sanmiguelia lewisii, PP34360. Apical portion of a nearly mature leaf, showing anastomosing vein bundles, apical vein fusion, and reformed secondary veins (possibly apex to leaf in Pl. 1, fig. c; see also figure 3i). -g. S. lewisii, SLIDE-118. Acetate transfer of a leaf, showing enlargement of dumbell-shaped stomata and small epidermal cells; x 370. -h. S. lewisii, SLIDE-118. Acetate transfer of a leaf, showing a cross vein with reticulate and scalariform elements, scalariform tracheids within larger veins, and epidermal cells elongated parallel between closely-spaced veins; x 90. -i. S. lewisii, SLIDE-118. Acetate transfer of a mature leaf fragment, showing abundant tertiary and quaternary veins, numerous cross veins (see also figure 3g-3h), and resin bodies (arrows); relative orientation unknown; x 3.7, note scale.

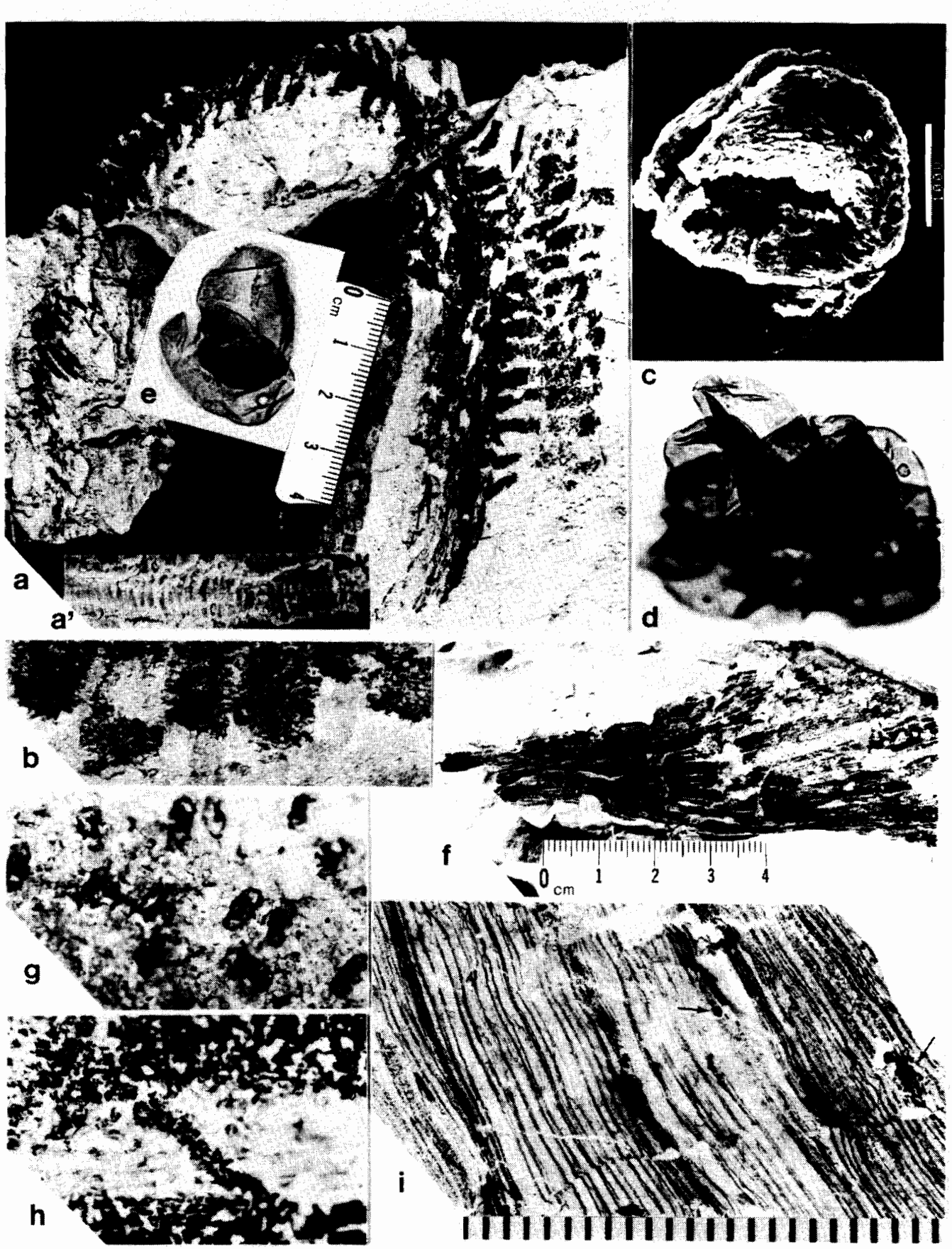
a
a'
b
c
d
e
f
g
h
i
0 cm 1 2 3 4

Plate 4, figs. a-h. Synangispadixis tidwellii Cornet sp. nov.; fig. i. Sanmiguelia lewisii Brown. -a, S. tidwellii, HYPOTYPE: PP34323. Distal end of a terminal inflorescence, overlapping distal portion of a large torn vegetative leaf (spathe?). -b. S. tidwellii, PP34322. SEMG of a nearly mature biloculate microsporophyll, with pollen masses exposed where endothecial layer has been removed; inset (b') showing enlargement of surface of endothecial cells with "waxy" beads of degraded cuticle on top; scale 100 um long. -c. Enlargement of specimen in fig. b, showing a cleft separating the two pollen masses, remnants of a tapetum overlying the pollen, and an endothecial layer on top; scale 10 um long. -d. S. tidwellii, PP34322. SEMG enlargement of a pollen mass to another microsporophyll, showing Übish bodies and tapetal debris covering immature monosulcate pollen, with granular intrastructure of wall showing through imcompletely formed tectum (compare with Pl. 3, figs. d-e); scale 10 um long. -e. SEMG enlargement of endothecial cells in wall to microsporophyll in fig. f (lower central); note mosaic intracellular structure; scale 10 um long. -f. S. tidwellii, PP34327. SEMG of transfer preparation to counterpart of specimen in Pl. 3, fig. b, showing paired, dehisced microsporophylls, each with only one pollen chamber at maturity; x 56.5. -g. S. tidwellii, PP34322. SEMG of microsporophyll, showing adaxial suture, enlarged endothecial cells flanking suture, tapering base, and portion of cuticle to axis; same scale as fig. h, x 200. -h. S. tidwellii, PP34322. Different view of same specimen in fig. g, showing an epidermal cuticle extending up from axis onto base of microsporophyll, and a thinner, more easily damaged wall layer between base and apex; scale 100 um long. -i. Sanmiguelia lewisii. Two macerated tracheids with circular bordered pits from the wood of main axis (figure 2a); x 300.

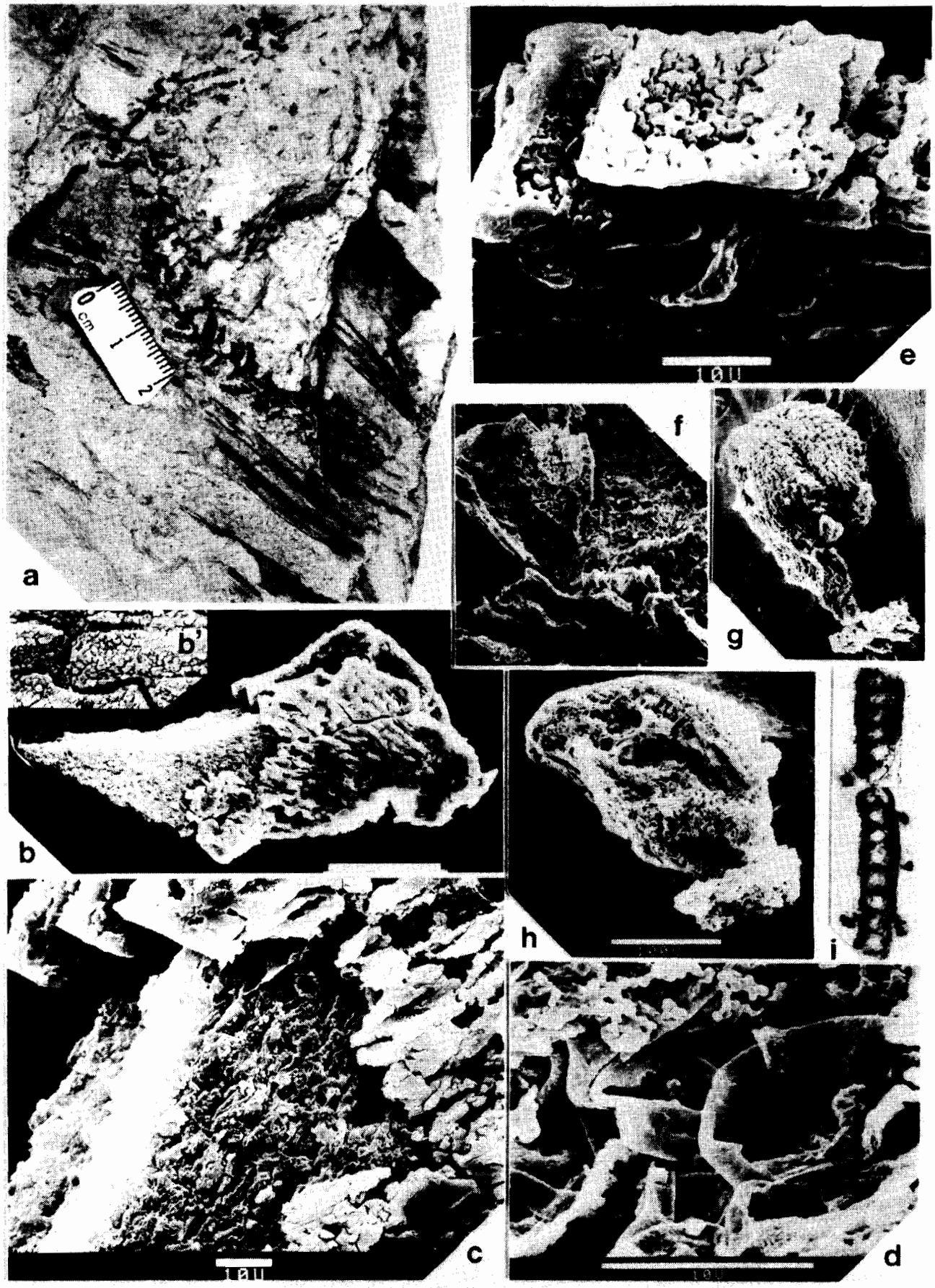
a
0 cm 1 2
b'
b
c
d
e
f
g
h
i

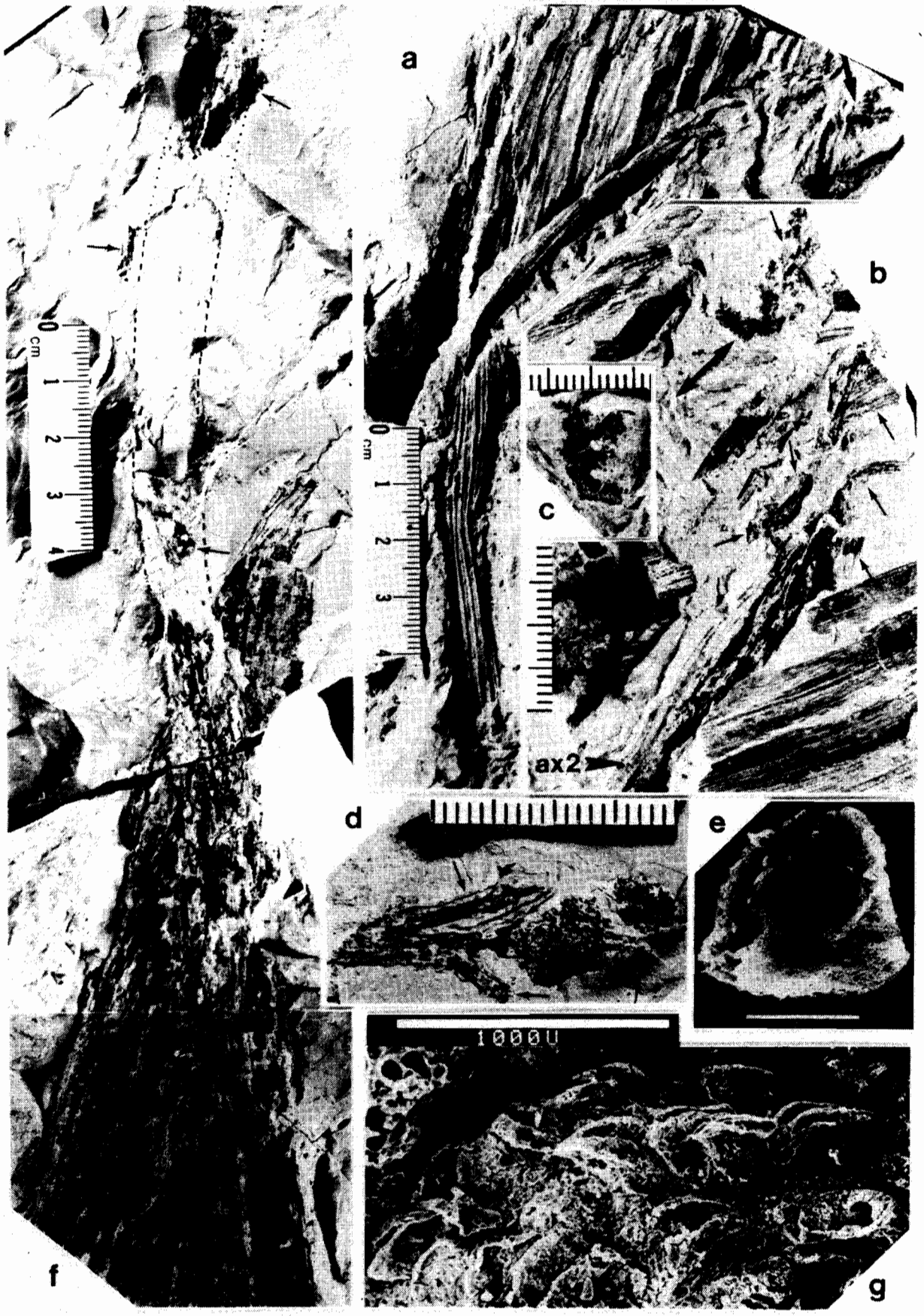
a
b
c
d
e
f
g
0 cm 1 2 3 4
0 cm 1 2 3 4
ax2
1000U

Plate 6, figs. a-c; g-k. Axelrodia burgeri Cornet sp. nov.; d-f. Nemececkigone fabaforma Cornet sp. nov. -a. A. burgeri, HOLOTYPE: PP34316. Distal portion of infloresence axis, showing long pointed sheathing cataphylls on the main axis, portions of secondary branches diverging from the main axis, flower-like units terminating secondary branches, and megasporophyll subunits borne on tertiary branches, along with their conspicuous digitate perianth parts (see figures 7c and 8a); same scale as in fig. b: x 1. -b. A. burgeri, HOLOTYPE: PP34317. Continuation of main axis 4 cm below base of specimen in fig. a, showing a shorter pointed parallel-veined bract with sheathing base; a second bract (arrow) exposed on opposite side of specimen; scale in mm. -c. A. burgeri, HOLOTYPE: PP34316. Dorsal view of an isolated carpel-like megasporophyll from counterpart to fig. a, showing bilobed stigma-like apex, paired shoulder pockets, and two anatropous ovules near torn base; striate surface pattern due to dense covering of long epidermal hairs (see figure 5c); scale in mm. -d. N. fabaforma, HYPOTYPE: PP34330. Plaster cast to mold showing chalazal end of right-handed seed, one side more convex than the other, hilum scar, and adjacent micropylar pit; same scale as fig. f: x 2. -e. N. fabaforma, HOLOTYPE: PP34329. Distal view of natural cast, showing one side flatter than the other and a median break that follows a median suture between opposite halves of seed coat; same scale as fig. f: x 2. -f. N. fabaforma, HOLOTYPE: PP34329. Side view of convex side (see figure 5b for labels); scale in mm. -g. A. burgeri, HOLOTYPE: PP34316. Enlargement of a nearly mature solitary megasporophyll subunit in fig. a, showing adjacent secondary axis, subtending conduplicate bract, and the compressions to a pair of developing seeds enclosed within the megasporophyll (see figure 5a and Pl. 7, fig. k for enlargement of stigma-like apex); same scale as in fig. h: x 2. -h. A. burgeri, HYPOTYPE: PP34320. Two adjacent, immature solitary megasporophyll subunits, showing inner and outer perianth parts, a subtending conduplicate bract, and location of a stamen-like organ (see figures 5e and 5f); scale in mm. -i. A. burgeri, HYPOTYPE: PP34321. Enlargement of a carpel-like megasporophyll from flower-like unit in fig. k (see figure 5d and Pl. 7, fig. e); x 4. -j. A. burgeri, HYPOTYPE: PP34321. Enlargement of cross section through stigma-like apex to a megasporophyll, showing u-shaped stylar canal (from Pl. 7, fig. e; comp. figure 7a); x 4. -k. A. burgeri, HYPOTYPE: PP34321. One side of a well-preserved flower-like unit, showing ten megasporophylls overlain by five perianth parts, a pair of adjacent ovules within one sediment-filled ovary, cross section of the secondary axis, and several solitary megasporophyll subunits, one of which is attached to a tertiary branch (see figure 5g); scale in mm. -l. Direct view of base to flower-like unit in fig. k (small arrows) and organic connections between flower base, secondary axis (ax2), and tertiary axis; x 2. Index to abbreviations: an, stamen-like organ; ax1, primary axis; ax2, secondary axis; ax3, tertiary axis; b1, bract or cataphyll along primary axis; b2, conduplicate bract subtending megasporophyll units and subunits; fr, fern rachis with pinnules; ms, individual megasporophyll; ms*, very immature megasporophyll; ms+, base to megasporophyll; ov, ovules; p1, inner entire hairy bract; p2, outer glabrous digitate bract; sd, seeds; st, bilobed stigma-like apex.

Plate 7, fig. -a. S. tidwellii, HOLOTYPE: PP34322, SLIDE-109. Two pollen masses isolated from one microsporophyll, with pieces of septum (black) still attached; 348 um and 366 um long; x 125. -b. S. tidwellii, HOLOTYPE: PP34322. SEMG of a microsporophyll broken open to reveal two pollen masses separated by a septum with a distinctive amorphous structure; scale 100 um long. -c. A. burgeri, HOLOTYPE: PP34316. Epidermal hairs and cuticle to megasporophyll; 400-450 um long, 12-22 um wide; x 100. -d. A. burgeri, HYPOTYPE: PP34321. End view of flower-like unit, showing apical end of one megasporophyll, and cross sections of several broken megasporophylls, one of which contains two adjacent ovules in a sediment-filled ovary (see figure 5g); scale in mm. -e. A. burgeri, HYPOTYPE: PP34321. Distal view of squashed flower-like unit in fig. d, showing about eighteen carpel-like megasporophylls, one of which contains two mature seeds; same scale as fig. d: x 2. -f. N. fabaforma, HYPOTYPE: PP34331. Chalazal view of a distorted seed, showing hilum scar, curved suture between seed coat halves, and position of micropylar pit (arrow); same scale as i: x 2. -g. N. fabaforma, HYPOTYPE: PP34332. Lateral view of flat side of a large right-handed seed, showing some striations on inside of seed coat; chalazal surface missing; same scale as fig. i: x 2. -h. Distal view of seed cast in fig. g; larger of two cotyledons filled convex side of seed; x 2. -i. N. fabaforma, PP34333. Carbonaceous remains of half a seed coat (convex side), indicating manner of germination; both top and side view shown; scale in mm. -j. A. burgeri, HYPOTYPE: PP34321. Enlargement of portion of fig. e, showing prominent keel at one end of an enclosed seed, and apical portion of an immature megasporophyll with indication of a ventral suture (arrows); x 4. -k. A. burgeri, HOLOTYPE: PP34316. Enlargement of the megasporophyll in Pl. 6. fig. g, showing apical stigma and impressions of two seeds (preserved as compressions on counterpart); scale in mm. -l. N. fabaforma, HYPOTYPE: PP34335. Carbonaceous remains and cast of embryo inside one seed; see figure 7b for details; scale in mm. -m. S. lewisii, SLIDE-118. Enlargement of actinocytic stomata (see figure 3j) and tracheids with reticulate pitting in a quaternary vein; x 370. -n. S. lewisii, SLIDE-118. Enlargement of epidermal trichomes of leaf, showing a 35 um long dendroid trichome (see Figure 31) and a single hair; x 625. hr, epidermal hair; kl, keel or ridge; ov, ovules; po, pollen mass; sd, seed; se, septum; st, stigma; tc, dendroid trichome.

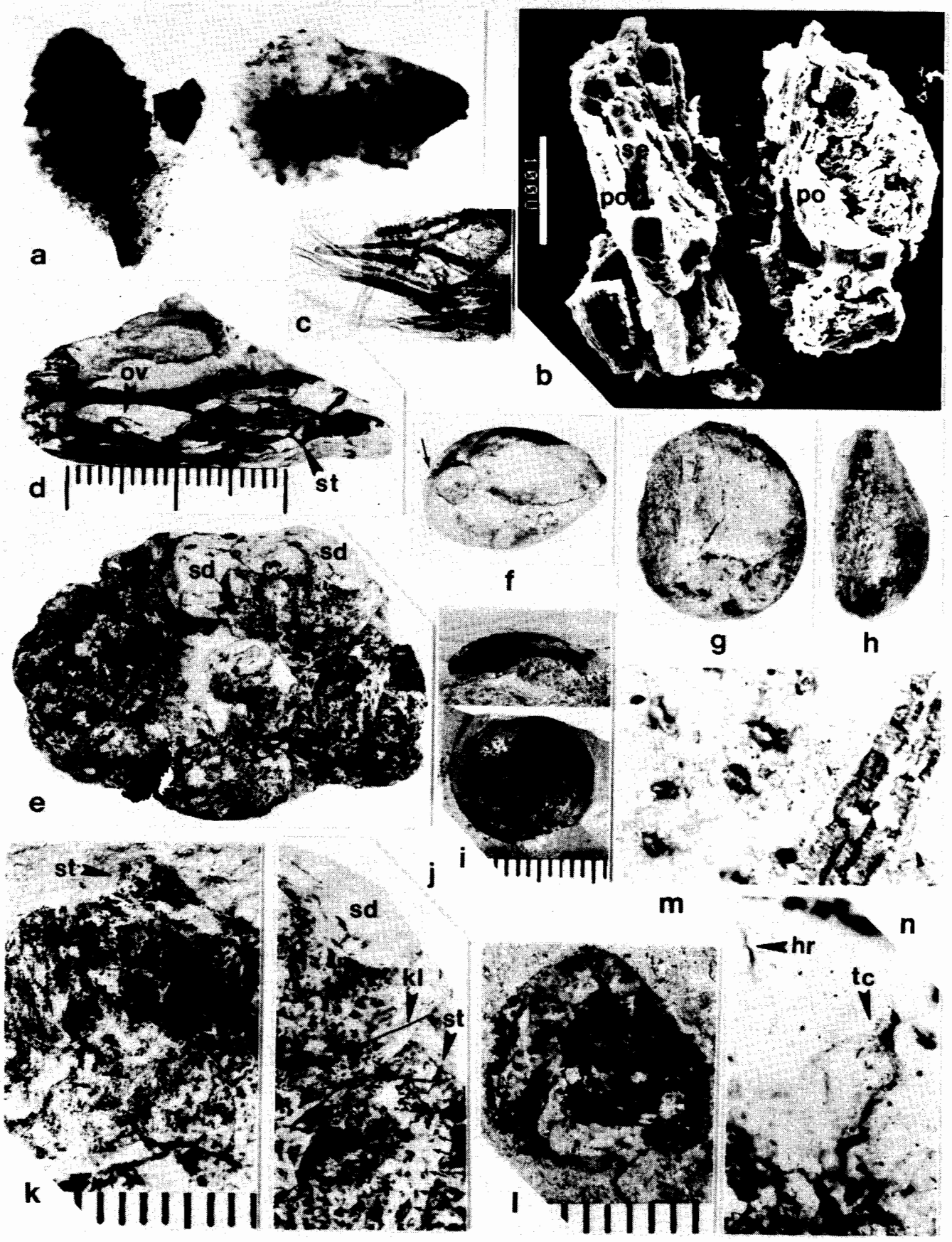
a
b
c
d
e
f
g
h
i
j
k
l
m
n
ov
st
sd
sd
se
po
po
st
sd
kl
st
hr
tc

Plate 8, figs. a; d-i. Sanmiguelia lewisii Brown; figs. b-c. Axelrodia burgeri Cornet sp. nov. -a. S. lewisii, PP34355. Limonitic petrifaction of root, showing portions (arrows) from which thin sections were made: Pl. 2, figs. c-e; scale in mm. -b. A. burgeri, HOLOTYPE: PP34316. Counterpart to specimen in Pl. 6, fig. a; enlargement of a disaggregated flower-like unit showing three hairy carpel-like megasporophylls (largest arrows), part of a simple hairy bract (intermediate size arrow), and portions of several glabrous digitate bracts (smallest arrows); the megasporophyll in the lower right corner is enlarged in Pl. 6, fig. c; scale in mm. -c. A. burgeri, HOLOTYPE: PP34316. Counterpart to specimen in Pl. 6, fig. a; enlargement of perianth parts to a large flower-like unit (covering most of field) and an immature flower-like subunit (largest arrow), showing a simple hairy bract (intermediate size arrow) and portions of several glabrous digitate bracts (smallest arrows); scale in mm. -d. S. lewisii, PP34340. Pith cast from distal part of stem lacking secondary xylem, showing successive, spirally-arranged lenticular parenchymatous gaps separating impressions of individual protoxylem bundles that surrounded the pith; note that protoxylem bundles appear to terminate at the acuminate ends of interfascicular gaps, which may represent leaf gaps; scale in mm. -e. S. lewisii, SLIDE-S16. Transverse section of primary and secondary xylem adjacent to pith (largely replaced by sediment), showing a series of closely-spaced endarch primary xylem bundles separated by probable uniseriate gaps or rays (ur) and widely-spaced gaps of probable multiseriate rays (mr), remnants of possible medullary vascular bundles in the pith (small arrows), and vesselless secondary xylem radiating outward from a zone of smaller tracheids peripheral to the metaxylem; x 32. -f. S. lewisii, SLIDE-128. Transverse section of secondary xylem, showing at least two uniserate rays traversing from left to right, and rows of tracheids (not fiber cells), whose walls have been thickened by invasive tyloses; x 133. -g and h. S. lewisii, SLIDE-128. Enlargements of secondary xylem showing uniseriate rays flanked by tracheids containing thick-walled tyloses - a possible wound response to damaged stems or the loss of leaves; tyloses indicate the presence of abundant wood parenchyma and companion cells; x 160. -i. S. lewisii, SLIDE-125. Composite photographs of a tangential section through secondary xylem, showing a tall massive multiseriate ray with an enclosed circular leaf trace near its base; uppermost photograph placed to the left to show how these massive rays occur in parallel groups; adjacent rays join in areas where tracheids locally disappear between them (white arrows); x 40.


a
b
c
d
e
f
g
h
i
0
cm
1
2
mr
ur
ur
ur
ur
mr
mr

Plate 9, figs. a-i. Zamiostrobus virginiensis Fontaine 1883 or Primaraucaria wielandii Bock 1954 sensu lato, Productive Coal Measures, Richmond Basin, VA. -a. TYPE A fruiting structure, ANSP #200220C (3953). Impression of fruiting head with spiral phyllotaxis of megasporophyll subunits, each showing folded impression of a subtending bract (b2) and an apical scar (st) to a stigma-like process; scale in mm. -b. TYPE A fruiting structure, ANSP #200221 (3961). Compression of a fruiting head (mss) terminating a long reproductive axis, possessing numerous spirally arranged bract-shaped leaves (b1); * indicates position of portion of compression removed for study (see figure 9a for a reconstruction); scale to right in mm: x 2. -c. TYPE A fruiting structure: Paired cuticles of subtending bract from specimen in fig. b (*); x 1,250. -d. TYPE A fruiting structure: Main axis and base to one carpel-like megasporophyll subunit (ms), showing diverging secondary branches (ax2) and possible base to subtending bract (b2?); from * in fig. b (see figure 10g); x 3.5. -e. TYPE A fruiting structure: Aborted, 250 um wide, anatropous ovule attached to cuticle of ovary wall; from * in fig. b; x 112. -f. TYPE A fruiting structure: Immature, 2.6 mm long seed removed from an ovary, showing micropyle (mi) adjacent to hilum (hi) and strongly recurved embryo body; from * in fig. b; x 20. -g. TYPE A fruiting structure: Nearly mature, 2.8 mm long seed with a thick wrinkled seed coat, showing only two small pits or depressions at one end and no functional micropyle or obvious hilum scar; from * in fig. b; x 18. -h. TYPE B fruiting structure, ANSP #200220A (3962). Compression of a fruiting head composed of numerous pedicellate carpel-like megasporophyll subunits (ms), collectively subtended by large latrorse laminar stamens (11s); see figures 9b and 10h); scale to left in mm: x 2. -i. TYPE B fruiting structure: Distal end of a megasporophyll in fig. h, showing pore-like opening (st) that may represent the base to a deciduous stigma; x 16.6.

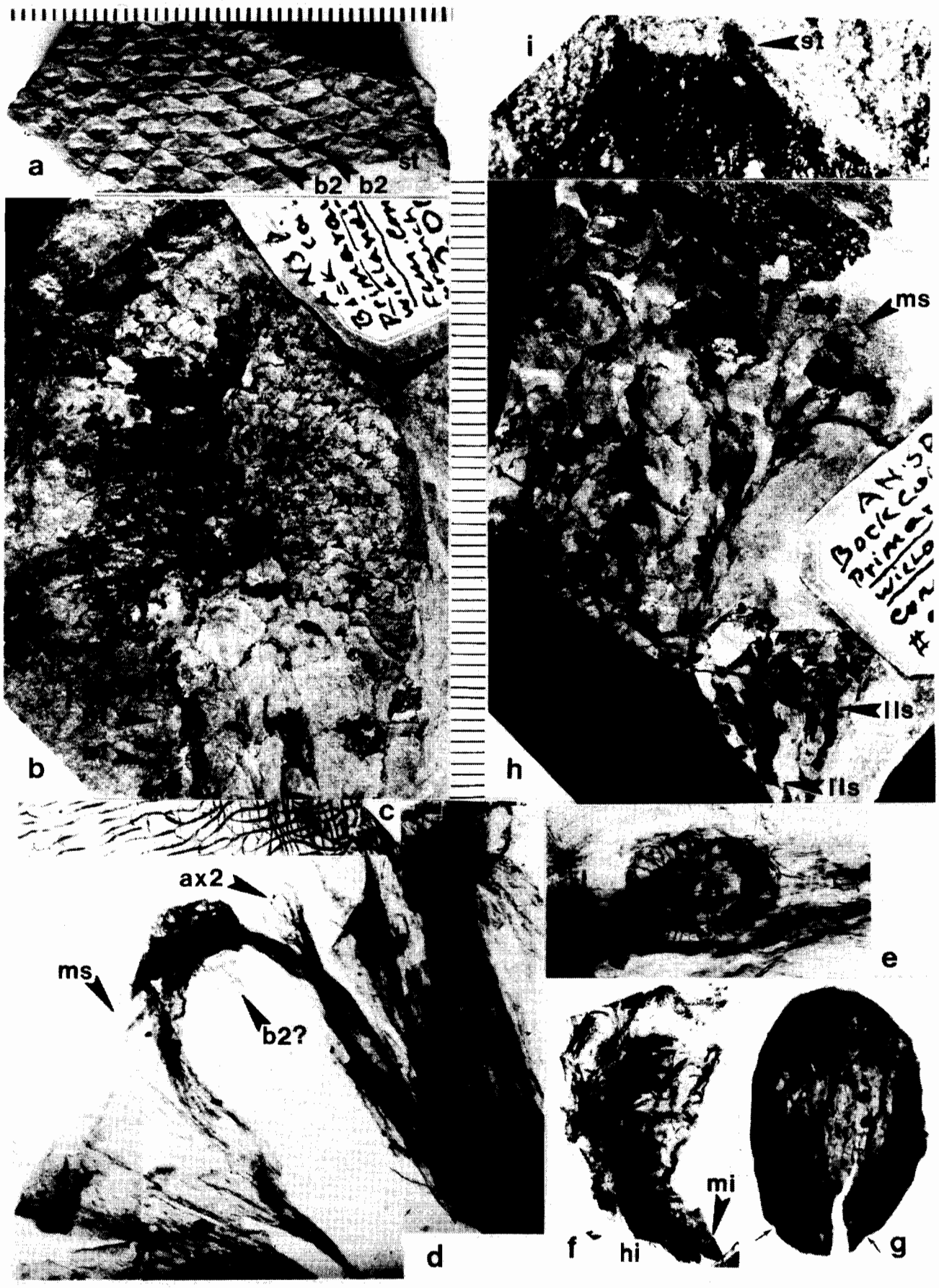
a
st
b2
b2
b
c
i
st
ms
h
lls
lls
ax2
ms
b2?
d
e
mi
f
hi
g